Anti-Slug Control and Topside Measurements for Pipeline-Riser Systems

Håkon Olsen

May 30, 2006

Abstract

The possibility of using topside measurements in anti-slug control for a pipeline-riser system is studied. Such systems have limited bandwidth due to right half plane zeros in the top-side measurement transfer functions. Remedies to this limitation are discussed as well as the inherent limitations in performance.. A cascade controller for anti-slug control based on top-side measurements is designed using a combination of linear controller design techniques and nonlinear simulation. Cascade control is also tested experimentally on a mini-plant.

KEYWORDS:
- Nonlinear systems, Two-Phase Flow, Cascade Control, Experimental Verification, Design Criteria, Performance Limitations.

To Maren, my girlfriend and soulmate.

Preface

This work is the culmination of my studies at the Norwegian University of Science and Technology. I would like to thank my supervisors, PhD student Heidi Sivertsen and professor Sigurd Skogestad for fruitful discussions and advice. I also want to show my appreiciation to professor Heinz Preizig, who lectured in my first control course, for opening my eyes to the world of control engineering. During the work, I have gotten very good help from the university's technical personnel, especially Mr. Frode Sundset and Mr. Odd Ivar Hovin.

Contents

Chapter 1

Introduction

The phenomenon of pipeline-riser slugging has long been though of as an inherent part of the nature of multiphase flow, and that this has to be accepted. In order to avoid problems due to varying flow in downstream equipment, large slug catchers have traditionally been built at the end of the line. This has several downsides; it puts a lower bound on the operating pressure of the pipe, which again limits the flow from the reservoir. It also increases the mechanical wear of the pipeline due to large oscillations in pressure. And also important; the capital and maintenance costs of a slug catcher are relatively large.

Another traditional method for avoiding problems due to slugging, is to choke the flow using the valve. If the valve opening is kept very low, the slug flow will cease. This too, of course, comes at the expense of higher operating pressure.

It has been shown that the natural flow pattern at a certain valve opening can be changed using feedback control, see for instance the PhD thesis of Storkaas (2005). This is fundamentally a different approach than the two traditional methods; control moves the flow regime boundaries in the flow map and thereby causes the flow to take place in a flow regime that is less problematic. This has been implemented in offshore applications using upstream measurements. The aim of this work is to develop anti-slug feedback control using topside measurements.

1.1 Pipeline-Riser Slugging

The phenomenon of pipeline-riser slugging can mathematically be described as a limit-cycle; these are sustained periodic oscillations in a nonlinear system. Physically, the oscillations occur due to competing forces. Liquid flows into the riser and fills it up. Eventually the weight of the liquid in the riser becomes too high, and the pressure drop over the riser is not large enough to drive the flow. This blocking causes the gas below the riser to compress. Eventually the pressure upstream the riser low-end reaches the hydrostatic pressure due to the weight of the liquid in the riser, and the riser contents is blown out rapidly. Then the liquid starts to build up again, and we have a limit cycle.

Below a certain valve opening, the riser slugging does not exist. Here the flow is steady, but the pressure in the pipeline is considerably higher than what is wanted for optimal operation. This is the flow regime that is being used when the choke valve is kept at a low opening, as described above.

The point where slugging starts in open loop is called a bifurcation point. A bifurcation point is a point (a specific parameter value) where the qualitative behavior of a nonlinear differential equation system changes

markably, like the transition from an equilibrium solution to a periodic solution, see for instance (Verhulst, 1990).

It has been observed that an unstable equilibrium solution exists at the same boundary conditions as the limit cycle. This unstable equilibrium is the operating point we wish to stabilize using feedback control.

A well-known mathematical example of this kind of behavior is the van der Pol equation;

$$\ddot{x} + x = \mu(1 - x^2)\dot{x},\ \mu > 0. \tag{1.1}$$

We set the parameter to $\mu = 1$ and produce the phase image (figure 1.1). A closed orbit in the phase plane indicates the existence of a periodic solution. The system has an unstable equilibrium point at the origin; a perturbation of the state causes the system to go into the limit cycle. This is the same situation as in the riser slugging case.

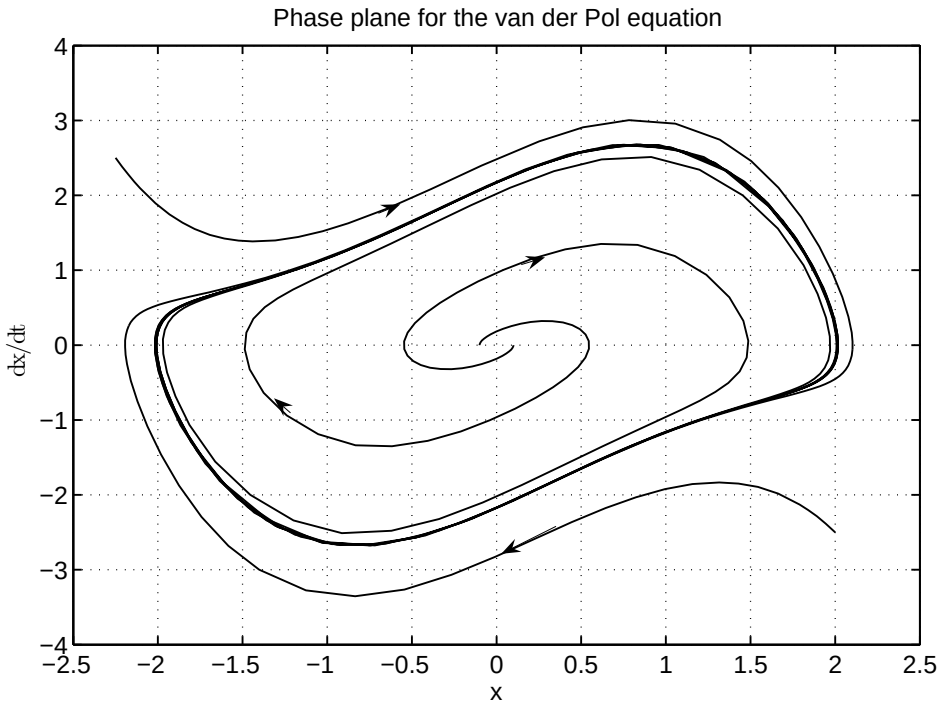

Figure 1.1: Phase plane of the van der Pol equation; a stable limit cycle

Some Remarks on Terminology

In the control literature, the notion of stability of a nonlinear system is mostly in the sense of Lyapunov; that is, stability is a property of equilibrium points in state-space. In terms of dynamical systems, a limit cycle is said to be stable if it is bounded and attractive. That means, a limit cycle is called stable if the oscillating system returns to the limit cycle after a perturbation, as in the van der Pol equation example (figure 1.1). In the sense of Lyapunov stability, however, every limit cycle is unstable.

The limit cycle which exists in the pipeline-riser system is attractive, and because it is a physical system it is of course also bounded. Therefore, the limit cycle is stable. We will, however, make the common control engineering use of the term stability and call the limit cycle unstable, which is correct in the sense of Lyapunov stability.

1.2 Previous work

Pipeline-riser slugging has been extensively studied from the fluid mechanics side, but the interest in this phenomenon from the control point of view is relatively new. The use of bottom-side measurements for stabilizing feedback control has been studied by Storkaas (2005), with focus on loop shaping controller design and linearization based controllability studies.

Storkaas has also treated the use of top-side measurements, and shown in simulations using simplified models that it should be possible to stabilize the flow using topside measurements only. He suggests using flow control in the inner loop and either choke pressure drop or the valve opening as controlled variable for the outer loop of a cascade control system.

Experimental work on anti-slug control has been done by different companies active in the offshore business. Statoil and Norsk Hydro have investigated the use of cascade control based on top-side measurements for anti-slug control, as well as industrial applications with upstream measurements since 2001, Godhavn et al. (2005).

They also suggest a very simple first-order linear model to describe the bottomside pressure dynamics near the pressure set-point.The model is meant to aid tuning of controllers.

1.3 The Storkaas Model for Severe Slugging

Most of the computer simulations and model based arguments in this work are done on basis of the Storkaas dynamic model for riser slugging. The Storkaas model is semi-empirical, and aims to model two-phase flow as a lumped system.

The model is fairly successful at modeling the slugging behavior, but its original form is in explicit differential-algebraic (DAE) form. Numerical simulations based on the DAE description damends a DAE solver. The problem is of index 1, and is solvable using one of the *ode23t* or *ode15s* routines in Matlab®.[1] or the freely available FORTRAN routines DASSL/DASPK.

The model assumes that the system can be described by coupling of three balance volumes. The bottom-side gas volume is assumed constant. The liquid holdup is modeled using one single volume for the pipeline and the riser. The top-side gas volume and the liquid volumes are assumed dynamic. There are three dynamic states in the model;

Liquid holdup m_L

Bottom-side gas holdup m_{G1}

Top-side gas holdup m_{G2}

[1] Matlab is a registered trademark of MathWorks Inc.

The state differential equations are as follows;

$$\frac{dm_{\mathrm{L}}}{dt} = \dot{m}_{\mathrm{L,in}} - \dot{m}_{\mathrm{L,out}} \tag{1.2}$$

$$\frac{dm_{\mathrm{G1}}}{dt} = \dot{m}_{\mathrm{G,in}} - \dot{m}_{\mathrm{G1}} \tag{1.3}$$

$$\frac{dm_{\mathrm{G2}}}{dt} = \dot{m}_{\mathrm{G1}} - \dot{m}_{\mathrm{G,out}}. \tag{1.4}$$

The two flow terms with index "in" are disturbances and are assumed constant. The flows out of the riser and between the feed pipeline and the riser are modeled by simple valve equations. The mixture density in the riser is treated as an algebraic state in the model. The most crucial point if the treatment of phase distribution. The traditional approach to this in fluid mechanics is to use a slip correlation to model the difference between the phase velocities.The Storkaas model uses an entrainment model from distillation theory to directly model the phase distribution in the riser.

The model has four tuning parameters, 3 valve constants to account for; flow of gas from pipeline to riser, liquid from pipeline to riser and one for the flow of fluid out of the riser. In addition to this, there is one parameter to tune the entrainment equation. Storkaas (2005) gives a procedure for tuning the model to experimental data.

1.4 Experimental

The experiments are performed with a mini-loop. The fluids used are water and air. This gives a density ratio quite different from that observed in petroleum systems, but the fundamental flow regimes observed are the same as known from oil/gas systems.

The loop is equipped with two pressure measurements (one at the base and one at the top) as well as a measurement of phase fraction. The phase fraction measurement is done using to light absorption measurement cells. The piping consists of see-through silicon rubber tubes, and the water has been colored with a blue coloring matter. The riser height is approximately 2.7 m. The light absorption sensors, from now on referred to as slug sensors, are situated 10 cm from each other just upstream the choke valve. The measurements are basically measuring if there is water in that section of the tube or not, and an average of the two measurements is used as an indication of phase fraction.

The water is circulated from a feed tank using a continuous pump. There is a flow rate measurement on the water feed to the system. Gas is supplied from an in-house pressurized air system. A simple process flow chart is shown in figure 1.2. Most of the time during this work, a gas flow measurement at the inlet has not been available, but a flow meter has been obtained towards the end of the project.

Data logging and controller implementation for the experimental rig are done using LabVIEW® [2]. The most important program constructs are given in appendix A. For a more detailed description of the sensors and equipment used with the mini-loop, see Baardsen (2003). The equipment which has been changed since then is the pump for circulating the liquid and the gas flow meter. In the current set-up a Grundfos (Denmark) resiprocating pump with a maximum head of 3.7 m is used and an air flow meter from the Cole-Parmer Instrument Company (USA).

[2] LabVIEW is a registered trademark of National Instruments Inc.

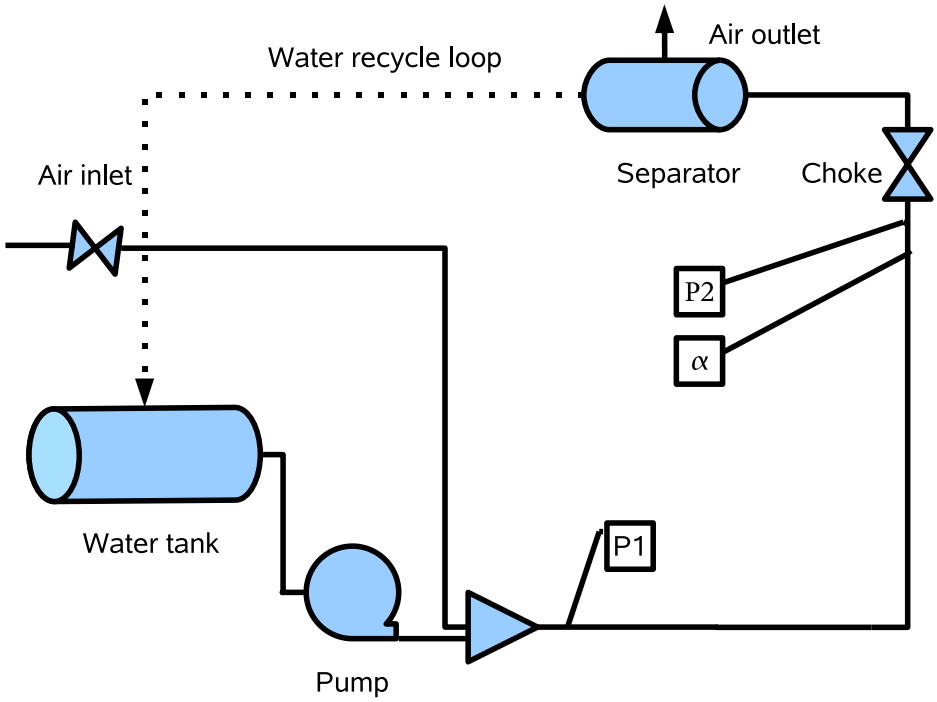

Figure 1.2: Flow chart showing experimental setup for anti-slug control experiments

1.5 Model Tuning

The Storkaas model is tuned to experimental data as described in the original work Storkaas (2005). The tuning procedure in short is; first, identify the bifurcation point. Then, tune on the parameter in the entrainment equation until the linearized system is marginally stable. After that, adjust other parameters until the amplitude and frequency of oscillations fit the experimental data.

Open loop experimental data

A series of experiments with open loop was performed to create data material for model tuning. A typical plot of upstream pressure P_1 as a function of time is shown in figure 1.3.

A bifurcation plot was created from the experimental data to aid model tuning. Figure 1.4 shows a bifurcation map of both experimental data (points) and from the tuned model (lines).

We observe that the model fit is quite good in open loop, especially at higher valve openings. Note also how the amplitude of the oscillations is not very dependent of the valve opening for $z > 30\%$.

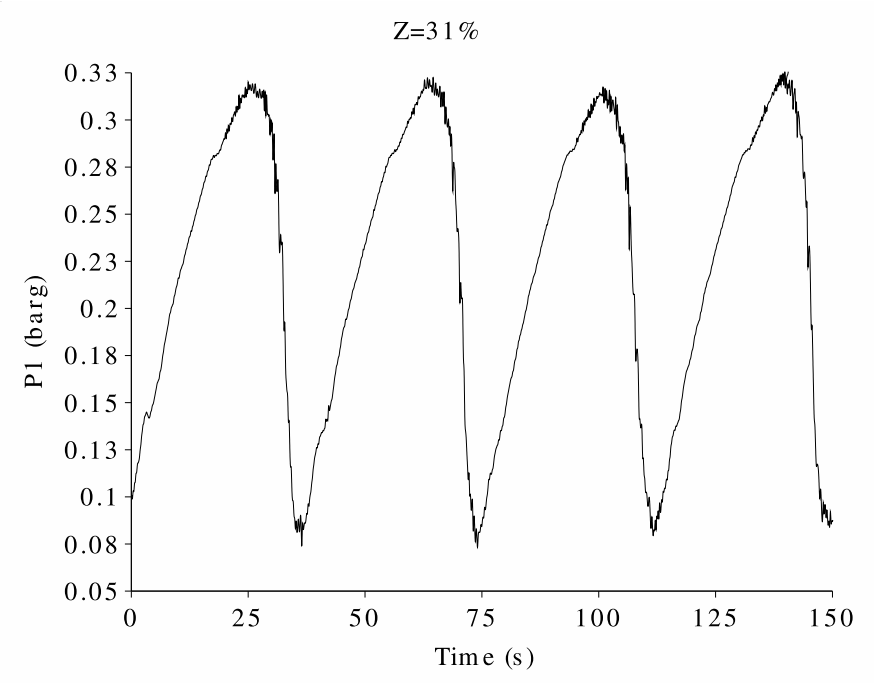

Figure 1.3: Typical behavior of P_1 at riser slugging conditions

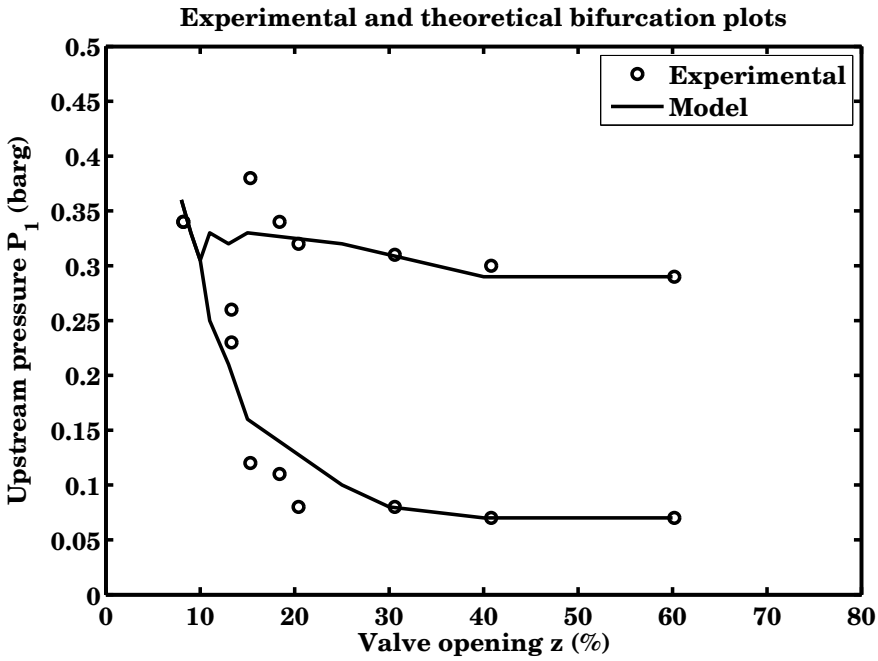

Figure 1.4: Bifurcation map for the riser slugging model (with experimental data)

Chapter 2

SISO Feedback Control

Riser slugging can be considerably reduced or even completely eliminated by feedback control. This chapter discusses controller design for anti-slug control where a bottom-side pressure measurement is available. The system is unstable, but minimum phase, and stabilization using a simple PI controller in a SISO loop is efficient and robust. Anti-slug control using bottom-side measurements has been tested successfully in several offshore applications.

The process model developed by Storkaas is nonlinear, such that linearization is necessary in order to apply standard design methods for PID control.The linearization point is the desired operating point, which is the unstable equilibrium solution of the model equations mentioned in Chapter 1.

2.1 Model Tuning and Linearization

Experimental data have been obtained from experiments with the system in open loop. The following data were collected. Using the data in Table 2.1, we estimate the bifurcation point to be at $z = 0.13$ (see also

z [%]	P_{min} [barg]	P_{max} [barg]
9	0.35	0.35
13.2	0.23	0.26
15.3	0.13	0.38
18	0.11	0.33
20	0.10	0.31
30	0.09	0.30
60	0.06	0.28

Table 2.1: Experimental data used to tune the Storkaas model; Bottomside pressure as function of valve opening in open-loop operation.

Figure 1.4) and with a bottomside pressure of 0.27 barg. At the same time we estimate the topside pressure to be 0.05 barg. Tuning on the entrainment equation parameter and the gas volume, we then manage to get a good fit to the open-loop data using the Storkaas model.An example of the open-loop behavior at z=0.20 is shown in Figure 2.1.

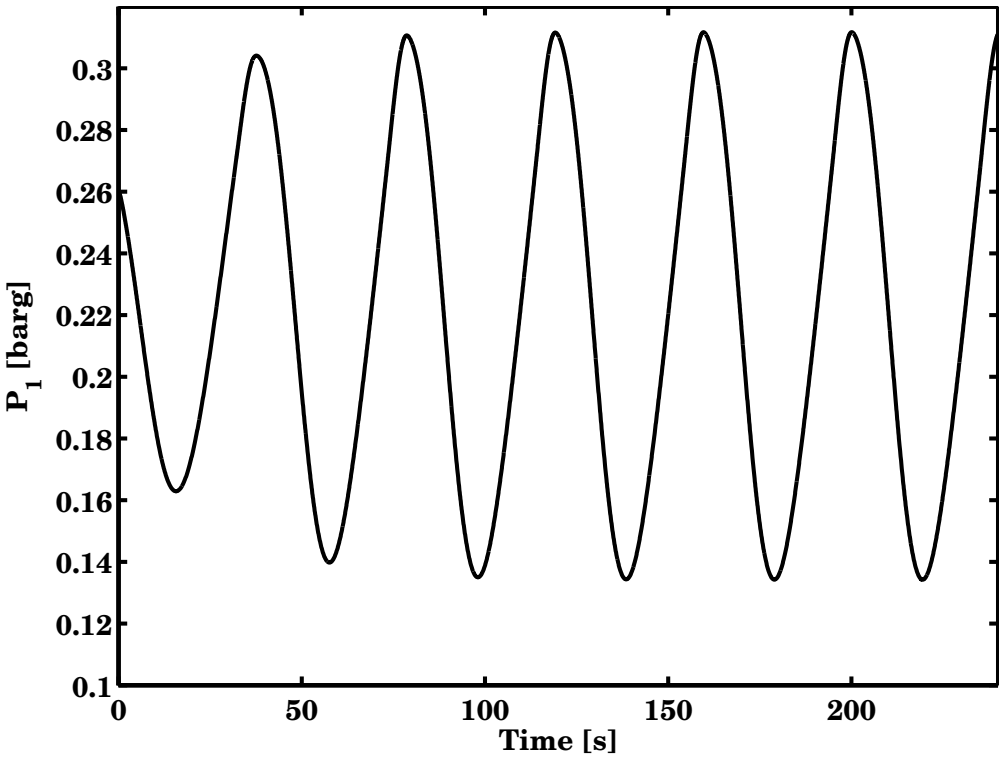

Figure 2.1: Simulation of pipeline-riser system in open loop at 20% valve opening.

The simulation gives a somewhat too small amplitude; the real signal has its minimum at $P_1 = 0.10$ barg, whereas the simulated signal has its minimum at $P_1 = 0.13$ barg.

Linearization

The process model is now linearized around the expected operating point. We assume that the operating pressure is 0.2 and that the topside pressure is 0.02 barg. Further, we expect the valve opening to be about 20%. This is well into the unstable area, as can be seen from Table 2.1. Linearization yields the following transfer function model for the seabed pressure;

$$G = \frac{P_1}{z} = \frac{-0.17s - 0.02}{s^3 + 3.73s^2 - 0.11s + 0.1}. \tag{2.1}$$

The system has a pair of complex-conjugate unstable poles located at $0.019 \pm 0.17j$ and one stable real pole at $s = -3.76$. The zero is located in the left half plane, at $s = -0.13$ and poses no serious problem for control.

2.2 Linear Controller Design and Simulation

The transfer function model developed in the last section will now be used to design a stabilizing controller. The control objective is to suppress terrain slugging, and to keep the system close to the given set point.

The control objective should be obtainable with a well-tuned PI controller. Integral action is needed to ensure good set point tracking. The transfer function of a PI controller with controller gain K_c and integral time τ_I is

$$K = K_c \left(\frac{\tau_I s + 1}{\tau_I s} \right). \tag{2.2}$$

We know that when the pressure is too high, the control valve should open. The control error is defined as

$$e(t) = r(t) - y(t), \tag{2.3}$$

where $r(t)$ is the set point and $y(t)$ the measurement. Therefore, we expect K_c to be negative. In order to go on with the design we form the closed loop transfer function from r to P_1;

$$G_c = \frac{K_c(-0.17\tau_I s^2 - (0.02\tau_I + 0.17)s - 0.02}{\tau_I s^4 + 3.73\tau_I s^3 - \tau_I(0.17K_c + 0.11)s^2 + (0.08\tau_I - 0.17K_c)s - 0.02K_c}. \tag{2.4}$$

The system has, as mentioned, a pair of complex-conjugate unstable poles. This imposes a lower bound on the bandwidth we can allow for effective control, see Skogestad and Postlethwaite (2005);

$$\omega_B^* > 0.67(x + \sqrt{4x^2 + 3y^2}, \tag{2.5}$$

where the complex-conjugate poles are located at $p = x \pm yj$. In our case, we then have that the closed-loop bandwidth should be greater than 0.21 rad/s. Matlab was used to calculate the frequency response of the closed-loop sensitivity function S,

$$S = (1 + GK)^{-1}, \tag{2.6}$$

and the design criteria chosen are;

- the bandwidth must be greater than 0.21 rad/s

- the sensitivity peak has a given upper bound; $||S(j\omega)||_\infty < 2$.

The design method is iterative, and different values of the controller parameters gave the following results in terms of bandwidth and sensitivity peak (Table 2.2).

K_c [bar]	τ_I [s]	ω_B [Hz]	$\|\|S(j\omega)\|\|_\infty$
-5	50	0.23	1.18
-5	25	0.23	1.25
-5	10	0.23	1.53
-10	10	0.30	1.63

Table 2.2: Performance indicators for PI controller design

The last design looks the most promising in terms of bandwidth, but it also has the most aggressive settings. The Bode magnitude plot of the sensitivity function for that control configuration is shown in Figure 2.2. Note the very low peak value of 1.63.

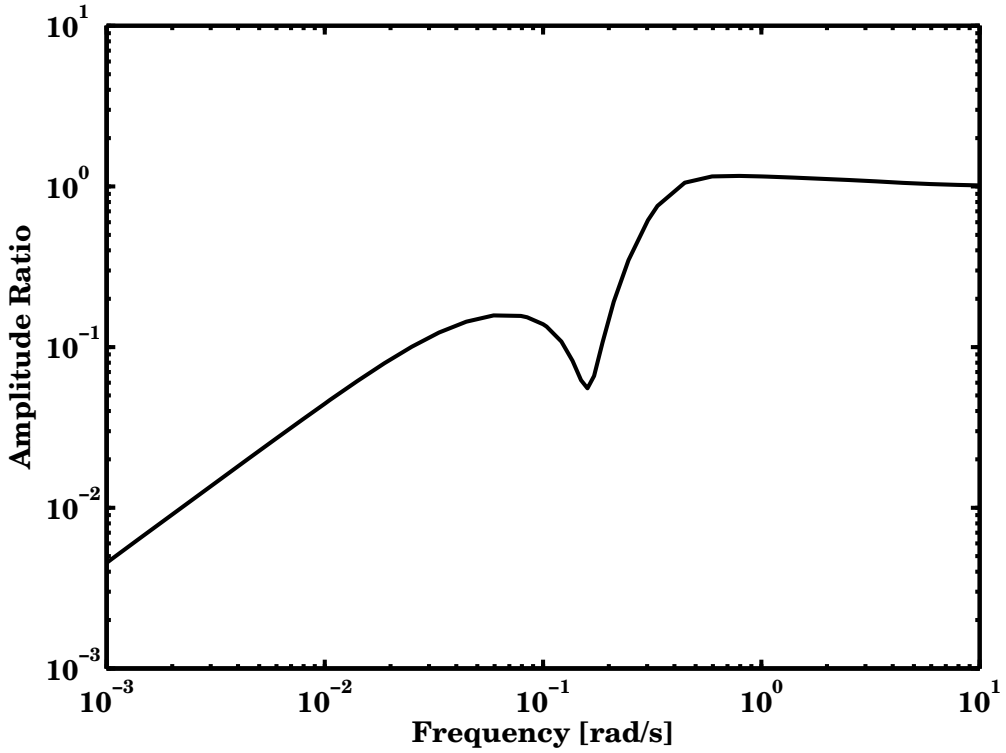

Figure 2.2: Bode magnitude plot for sensitivity function with $K_c = -10$ and $\tau_I = 10$.

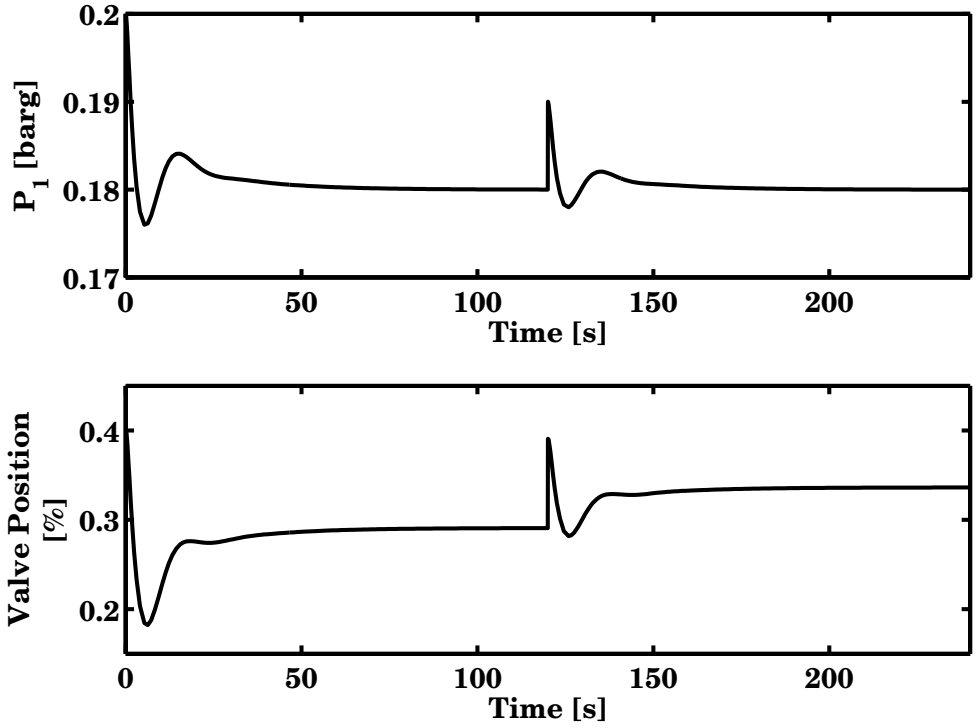

Figure 2.3: Simulation results of test case using PI control (linear model).

Linear Simulation

To confirm the design we now perform a simulation based on the PI controller with settings $K_c = -10$ and $\tau_I = 10$. We simulate a set point change from 0.2 bar gauge pressure to 0.18 bar gauge pressure at $t = 0$. After 2 minutes a disturbance of magnitude 0.01 bar is introduced in the measurement. The results are given graphically in Figure 2.3

2.3 Nonlinear Simulation of PI Control

A PI controller has been designed using linear methods. Now we want to test the performance of this controller using the nonlinear Storkaas model, which was also used to obtain the linear model by linearization.

The Storkaas model consists of three differential equations and a large set of state-dependent internal variables. The model contains several hard nonlinearities, and this causes the problem to be relatively stiff in certain ranges of the state-space. Therefore, the choice of the numerical method is important in order to obtain reliable results. The problem is here solved using the ODE23T routine in Simulink. The ODE23T routine can handle moderately stiff differential equation systems and also DAE systems. In the original implementation of the model, the DAE structure is used. Simulink is, however, not able to handle problems with a singular mass matrix, that is, problems on the form

$$\mathrm{M}\frac{dx}{dt} = f(x,t),$$

where M is a square singular matrix (it has zero rows for all algebraic equations).

The Storkaas model contains one algebraic equation. In the Simulink implementation of the model, the algebraic state is calculated iteratively from time step to time step, and in that way the problem with the mass matrix is solved. For details on the numerical considerations and on the model, see Appendix D.

Using the same test case as in the linear simulation, we discover that the controller is not able to handle a set point change from 0.2 to 0.18 barg. After the set point change, the instability occurs again. The result is shown in Figure 2.4. It seems the controller action is not fast enough to stop the limit cycle from reoccuring. The controller does, however, reduce the amplitude of the oscillations markably, as can be seen from comparison with data in Table 2.1 or from open-loop simulations with valve openings in the unstable region (where the limit cycle is the stable solution).

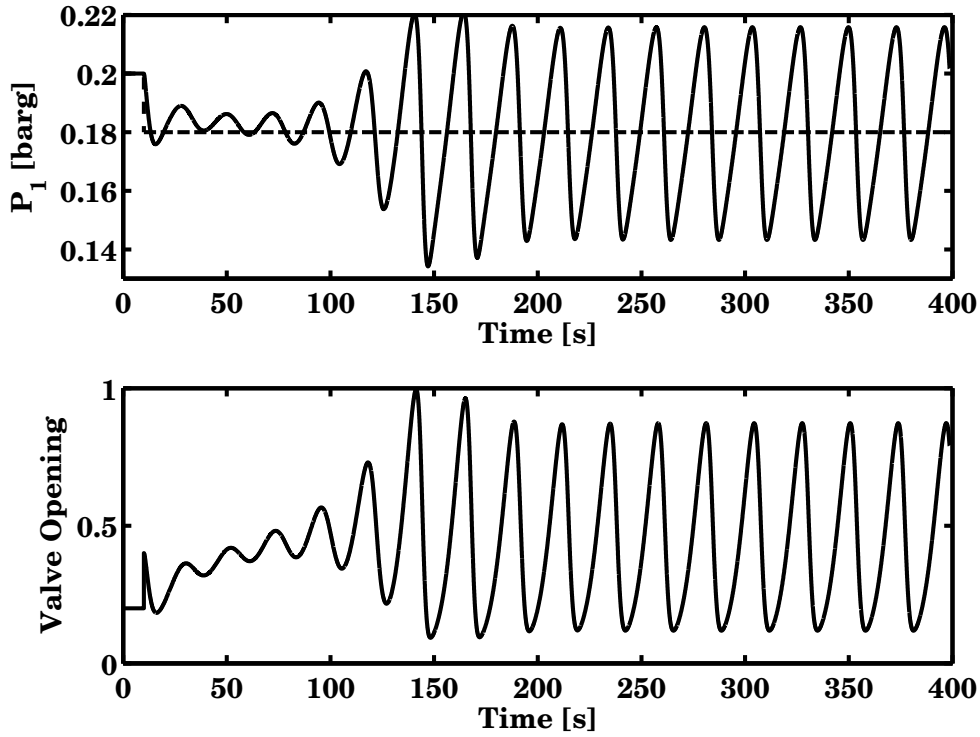

Figure 2.4: The design is not good for set point tracking due to nonlinear effects.

We now try to increase the gain in order to make the controller more efficient. Setting the gain to $K_c = -50$ yields a much better response, as can be seen from the simulation output shown in Figure 2.5. Note that the linear analysis indicated that this design has a lower sensitivity peak, which in general indicates better performance.

The model shows a very large valve opening, and it is experimentally not possible to stabilize the flow with such a high valve opening. This indicates that the tuning could be improved, because it is well possible to stabilize the process at pressures lower than 0.18 barg using much smaller valve openings than shown in Figure 2.5.

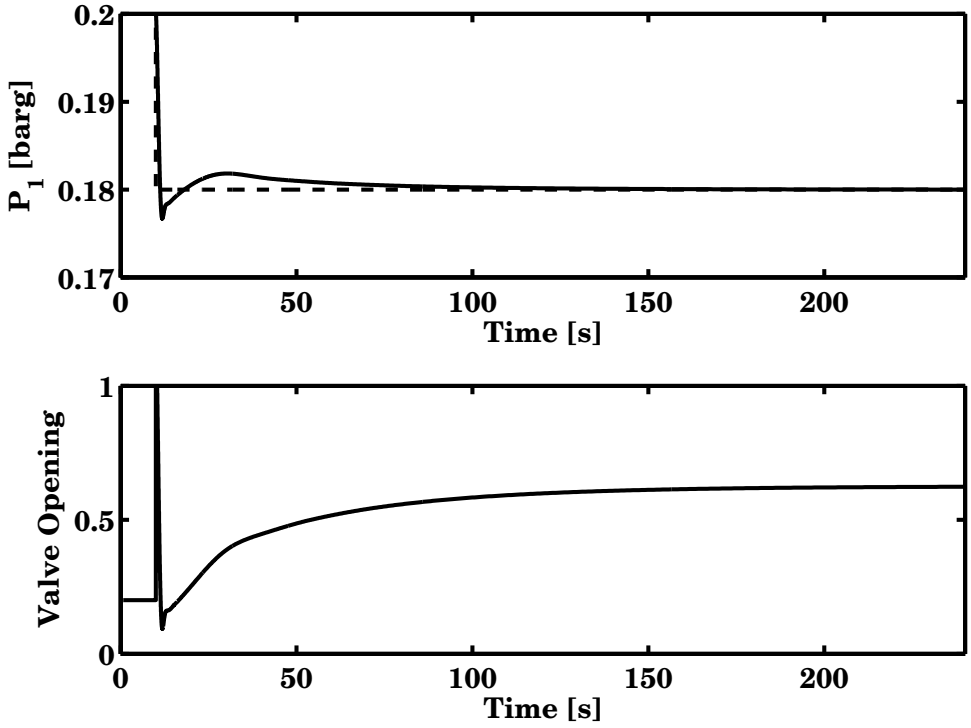

Figure 2.5: Increasing the gain allows for tight control

2.4 Experimental

Experimentally it has been shown that stabilization using a bottom-side measurement is easy. The process performs well under simple proportional control. Under feedback control the flow regime is changed. The flow pattern when the flow is stabilized is in the regime of hydrological slugging; much smaller and faster slugs. These are not a problem for the separator tank because the oscillations in flow are much faster than the residence time in the tank. Therefore, all of these high-frequency effects are completely levelled out by the capacity of the tank.

Proportional Control

A simple proportional controller was applied to the experimental mini-loop described in Chapter 1. The controller was well able of stabilizing the flow down to a set-point of 0.15 barg. Below that limit, the slugging reoccurred.

Setpoint tracking was good. The limit $P_1 = 0.15$ barg seems like a lower bound on effective stabilization using proportional control.This corresponds to an average valve opening of 26 % which is well into the open-loop unstable region, as seen from the data Table 2.1. The valve opening at the start of the experiment was 31%.

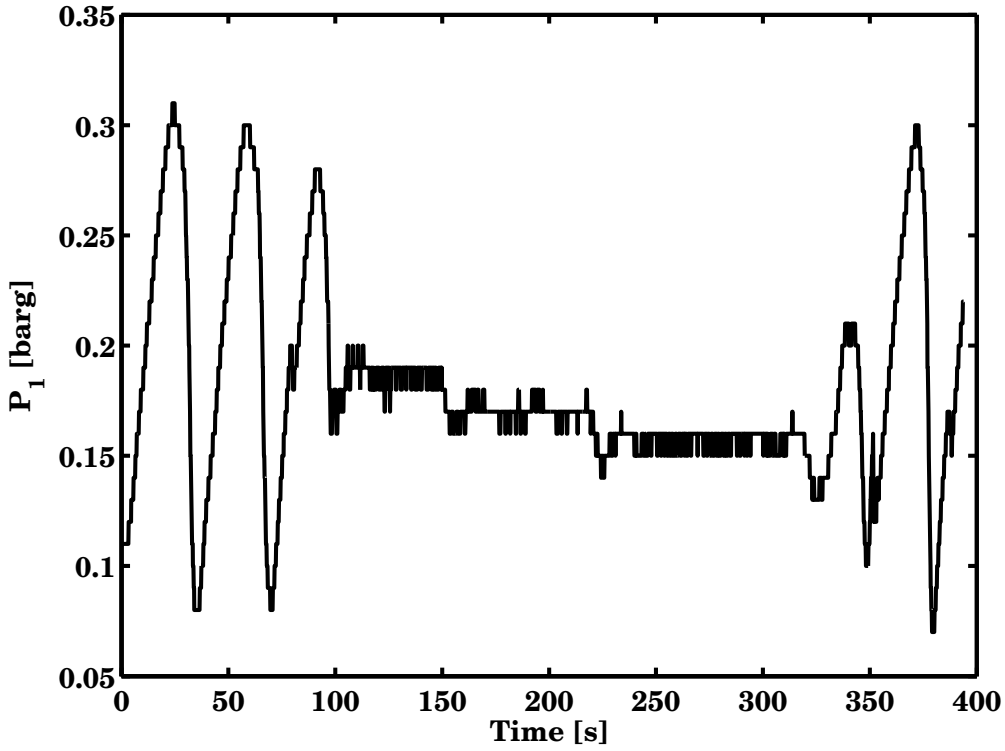

Figure 2.6: Experimental results; Proportional control with gain $K_c = -10$

PI Control

A proportional-integral mode controller was also tested with the bottom-side pressure. The controller has a simple anti-reset windup system obtained by resetting the integrand to zero if the controller output saturates. This is described in detail in Appendix A.

Using a PI controller with gain $K_c = -4$ and integral time τ_I, the tracking performance of the system was very good. The output and set point are shown in Figure 2.7.

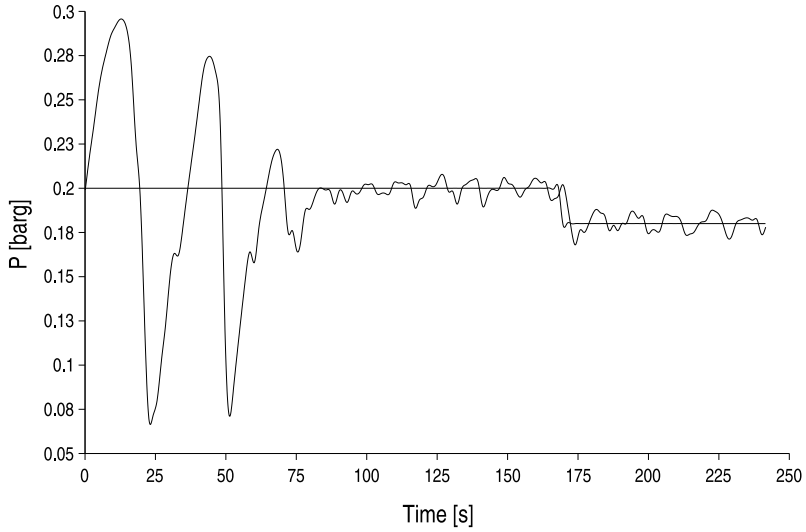

Figure 2.7: The tracking ability of the PI controller is very good.

The output usage is moderate due to the low gain, but note the large changes in controller output needed to stabilize the flow (Figure 2.8).

2.5 Summary

Stabilizing control using bottom-side pressure measurements has been discussed. Control using pressure measurements at the seabed level is not limited by non-minimum phase behavior and is a simple and robust solution to the riser slugging problem, as long as such a measurement is available. These claims are supported both by simulations and experiments

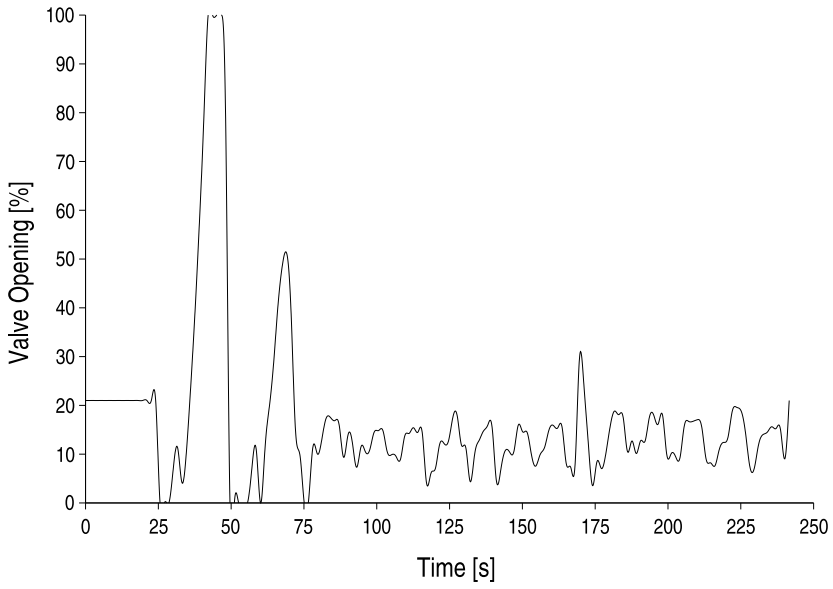

Figure 2.8: Output usage from PI controller.

Chapter 3

Topside Measurements: Limited Controllability

3.1 Introduction

When using topside measurements to control the system, we encounter fundamental limitations because of RHP zeros. In the laboratory system the available measurements are shown in Figure 1.2. The use of two independent measurements should be able of counter-acting the limitations of the RHP zeros, such that the system can be stabilized.

It has been shown by others that total volumetric flowrate can be used for control, because the transfer function of this measurement has no RHP zeros. It is possible to use a valve equation to estimate the flow, but for that we need a measurement or an estimate of the density of the fluid flowing into the choke valve. Inspired by the Bernoulli equation, we can hypothesize the following expression for the valve equation to use;

$$\hat{Q} = K(z, \alpha)\sqrt{\frac{P_2 - P_0}{\rho_T}}, \tag{3.1}$$

where P_0 is the separator pressure and ρ_T the density we need to estimate. In our case, P_0 can be assumed to be atmospheric, because the tank at the top has an open vent.

The valve constant is dependent on the valve opening, this follows from the valve characteristics. The valve constant will in general also depend on the fluid flowing through it. The phase distribution dependency is assumed to be much smaller than the effects of pressure and valve opening.

A mass flow meter for air has been ordered, but has not arrived before very late in the project; therefore it has until now not been possible to calibrate the valve equation for the gas flow.

The ρ_T estimate is calculated as follows;

$$\rho_T \approx \alpha_L \rho_L + (1 - \alpha_L)\rho_{G2}. \tag{3.2}$$

The measurement of phase fraction is based on light absorption in the fluid passing a sensor. The sensor is located just upstream the choke valve, see Figure 1.2. The measurement is problematic to use for control due to very large noise spikes. Using a smoothing filter helps, but comes at the expense of extra phase lag.

The gas density upstream the valve is also a dynamic quantity. It depends on the mass holdup of gas in the riser as well as the available volume. These quantities are unknown but determined by the states. Therefore, a state observer might help in generating the necessary information.

The first approach taken here is to assume that the gas density is constant. The error introduced by this should not be large, as the density of the two-phase mixture is completely dominated by the liquid even at very small liquid fractions. Around the stabilized operating point, the flow is not slugging, such that inaccuracies in volumetric flow calculations for pure gas flow should not be very important.

In the following, we look at non-minimum phase systems in general, and we will return to the slug flow case afterwards. The next chapter discusses the design and use of a valve equation for flow estimation.

3.2 Case Study: Controllability of a Non-Minimum Phase System

The characteristic limiting property of the topside measurement dynamics is the existence of RHP zeros. The following case study investigates the effect of RHP zeros on controllability and performance.

The following transfer function model of top-side measurements is used in the subsequent analysis;

$$G_1 = \frac{5(-4s+1)}{s^2 - s + 1} \tag{3.3}$$

$$G_2 = \frac{5(-6s+1)}{s^2 - s + 1}. \tag{3.4}$$

The system has a pair of complex-conjugate poles in the right half-plane (RHP), namely at $p_i = 0.5 \pm 0.87j$.

Performance Limitations on SISO Control

Intuition tells us that a SISO controller cannot stabilize the process, because the inverse response is slower than the instability; hence the instability is practically invisible to the controller when it occurs and the controller reacts to late. This is also seen in the real system where the instability is an attractive limit cycle. The controller action, when applied on basis of topside measurements is out of phase with the limit cycle. That means, that the use of SISO feedback control with topside measurements would rather further destabilize the process instead of forcing it to the sought-for unstable equilibrium solution.

State controllability is not of much use here, because a system might very well be state controllable yet inherently difficult to control efficiently in practice. State controllability does not take input limitations or causality in consideration, and for process control these are very important constraints on the controller design.

That RHP zeros limit the bandwidth of the system seems like an intuitive notion. Now let the sensitivity function be given by $S = (I + L)^{-1}$, with L defined as in Theorem 1. The following theorem quantifies the notion on sound theoretical arguments.

Theorem 1 (Waterbed formula)
Let L(s) be the loop transfer function of the feedback system. Suppose L(s) has a single RHP zero and N_p RHP poles. Then, for closed-loop stability the following integral equation must hold;

$$\int_0^\infty \frac{2}{z(1 + (\omega/z)^2)} \ln |S(\omega j)| \, d\omega = \pi \ln \prod_{i=1}^{N_p} \left| \frac{p_i + z}{\bar{p}_i - z} \right|.$$

□

.

For extensions and discussion of the theorem, see (Skogestad and Postlethwaite, 2005).

The result in Theorem 1 is often hard to apply in practice. A controller must be synthesized and then the waterbed theorem can be applied to assure stability. The resulting integral equation more often than not becomes too complicated to be of any convenience compared to using the poles of the closed-loop transfer function. The theorem can however be the starting point for development of bounds on the sensitivity function. It also shows that forcing the sensitivity function $|S(j\omega)|$ down in some frequency region, causes the sensitivity to increase in another frequency region.

Let w_P be a performance weight on the sensitivity function, as used in loop shaping controller design. Let the $\mathcal{H}_\infty$ norm be given as the infinity norm of a Hardy space, which is defined as follows (Young, 1988);

Definition 1 (Hardy spaces)
Let f be a function in L^2, where L^2 is the Hilbert space of Lebesgue square integrable complex-valued functions on the unit disk with pointwise algebraic operations and inner product defined by

$$(f, g) = \frac{1}{2\pi} \int_{-\pi}^{\pi} f(e^{j\theta}) \bar{g}(e^{j\theta}) d\theta.$$

Further, let $\hat{f}(n)$ be the n'th Fourier coefficient of f, given by

$$\hat{f}(n) = \frac{1}{2\pi} \int_{-\pi}^{\pi} f(e^{j\theta}) e^{jn\theta} d\theta.$$

Let $p = 2$ or $p = \infty$. The Hardy space H^p is the closed subspace defined as;

$$H^p : \{f \in L^p : \hat{f}(n) = 0, \ \forall n < 0\}.$$

□

The definition of the Hardy space given in Definition 1 does not have any practical meaning for the concept of controllability; all practically occurring signals belong to a Hardy space.

The infinity norm induced by the inner product on a Hardy space is called the $\mathcal{H}_\infty$-norm;

$$\mathcal{H}_\infty(f) = ||f||_\infty = \max_\omega \{f(\omega)\}, \tag{3.5}$$

which is simply the magnitude peak of the transfer function f.

Now we are ready to present a lower bound on the sensitivity. The following theorem is given by Skogestad and Postlethwaite (2005), please see the cited book and references therein for proof.

Theorem 2 (Sensitivity peaks)
Let the open-loop process be described by the transfer function $G(s)$. For each RHP zero z in $G(s)$ the following must hold;

$$||w_P S||_\infty \geq |w_P(z)| \prod_{i=1}^{N_p} \left| \frac{z + p_i}{z - p_i} \right|$$

where p_i are the RHP poles of the transfer function G(s). The weight w_P is the performance weight used in loop shaping design.

For the complementary sensitivity function, we have a bound for each RHP pole;

$$||w_T T||_\infty \geq |w_T(p)| \prod_{j=1}^{N_z} \left| \frac{z_j + p}{z_j - p} \right| |e^{p\theta}|,$$

where N_z is the number of RHP zeros, θ is the time delay. The bound is tight if the transfer function has only one RHP pole.

□

An often applied weighting function for the sensitivity is given by

$$w_P(s) = \frac{s/M + \omega_B^*}{s + \omega_B^* A}, \tag{3.6}$$

where ω_B^* is the required bandwidth, A is the low-frequency asymptote and M is the high-frequency asymptote.

What is the Best We Can Do with a PI Controller?

It is interesting to see what the best control we can obtain with a simple PI controller is. The first question is, whether it is possible at all to stabilize the process without using an improper controller (which is physically unrealizable). The answer based on intuition is "no", because the RHP zero lies further into the RHP than the unstable poles.

The transfer function for the PI controller is for the most common implementation;

$$G_c = K_c \frac{\tau_I s + 1}{\tau_I s}. \tag{3.7}$$

Then we obtain the following sensitivity function;

$$S = \frac{\tau_I(s^2 - s + 1)}{\tau_I(s^2 - s + 1) + 5K_c(\tau_I s + 1)(-4s + 1)}. \tag{3.8}$$

The first thing we do now, is to develop the lower bound on the sensitivity function magnitude, $|S(j\omega)|$. There is only one RHP zero in G_1, hence Theorem 2 guarantees a tight bound. The bound is given as

$$||S(j\omega)||_\infty \geq \prod_{i=1}^{N_p} \left| \frac{z + p_i}{z - p_i} \right|, \ \forall z \in \text{RHP}.$$

Inserting the values on the right-hand side, we obtain;

$$||S(j\omega)||_\infty \geq \frac{75^2 + 87^2}{25^2 + 87^2} = 1.61.$$

This peak is greater than 1, but does not seem very bad. However, there is no guarantee there exists a causal controller that can achieve anything close to this. For a linear system there will always exist a controller that can stabilize the system, if we allow the use of future information (future set point changes, for instance).

For a rigorous proof that the stabilization using a PI controller is indeed impossible, one could proceed by application of theorem 1, where one would have to show that the integral equation has an empty solution space. To show this is, however, very difficult because the integral has no analytical solution, or it is at least very hard to obtain.

The integral is improper because the limit is infinity. One option to prove inequality could be to show that the integral is divergent, whereas the right hand side of the equation is a finite number.

The simplest approach is taken here. Routh's stability criterion states (Seborg et al., 2004);

> Let the characteristic equation be written on the form $\sum_{i=0}^{N} a_i x^n$. If all coefficients are not positive or all negative, at least one root of the equation lies in the right half plane or on the imaginary axis [1]

Developing the closed-loop transfer function for a PI controller used with the process given by equation (3.3), we arrive at

$$G_{\text{closed}} = \frac{5K_c(\tau_I s + 1)(-4s + 1)}{\tau_I s(s^2 - 2 + 1) + 5K_c(\tau_I s + 1)(-4s + 1)}. \tag{3.9}$$

The characteristic equation is;

$$\tau_I s^3 - (20K_c\tau_I + \tau_I)s^2 + (5K_c(\tau_I - 4) + \tau_I)s + 5K_c = 0. \tag{3.10}$$

The Routh criterion allows us to state a sufficient test for instability as a system of inequalities. Assume that all coefficients of the polynomial equation (3.3) are positive. Then;

$$\tau_I > 0 \tag{3.11}$$
$$20K_c\tau_I + \tau_I < 0 \tag{3.12}$$
$$5K_c(\tau_I - 4) + \tau_I > 0 \tag{3.13}$$
$$K_c > 0. \tag{3.14}$$

If τ_I and K_c are positive, we have $20K_C\tau_I + \tau_I > 0$, which contradicts the inequality in (3.12). Next, assume that all coefficients are negative. Then, multiply the characteristic polynomial by (-1) and the same argument holds to prove instability. Hence, it is not possible to stabilize the system with a PI controller.

□

What Can be Obtained by Using Extra Measurements?

Feedback control cannot move zeros or eliminate time delays. This imposes serious limitations on stability and performance of closed-loop systems. A non-minimum phase system with large dead-time or zeros to the right of the fastest unstable pole is not possible to stabilize using a physically realizable controller.

[1] This follows from the sign rule of Descartes and in the Routh-Hurwitz stability criterion it is assumed that all coefficients have the same sign.

If we give up the SISO control paradigm and look at MISO controllers, the question is "how can extra measurements change the numerator dynamics?".

The answer is that the controlled variable can be selected to be any combination of the available measurements. The zeros of a transfer function are the roots of the numerator polynomial. Linear systems have the property of superposition, hence the input-output behavior of a linear combination of measurements is given by the linear combination of the individual transfer functions. Say we have the measurements y_1 and y_2, the scalar input u, and transfer functions from u to y_1 and y_2 called G_1 and G_2 respectively. Now we want to form a new controlled variable $\xi = y_1 + \gamma y_2$, where γ is a constant. Then, the transfer function from u to ξ is $G_\xi = G_1 + \gamma G_2$. Assume further that the transfer functions G_1 and G_2 have no time delays, and that the numerator polynomial of transfer function j can be written;

$$\mathcal{P}_{Nj} = \sum_{k=0}^{N} a_k^j s^k = 0,$$

where N is the degree of the numerator polynomial. The zeros of the transfer function from u to ξ are given by the roots of the following polynomial equation;

$$\mathcal{P}_{N_1,1} + \gamma \mathcal{P}_{N_2,2} = 0.$$

When designing a MISO controller based on some linear combination of measurements, a choice of design objective must be made for the linear combination. For practical controllability we should choose a linear combination such that the zeros are located at least to the left of the fastest unstable pole in the complex plane. If a RHP zero lies to the right of the fastest unstable node, the instability is not observable. In addition to this, we must demand that the slowest zero is sufficiently far from the fastest unstable pole. If these dynamic nodes are close to each other, the sensitivity peak will approach infinity and control is lost. This follows directly from Theorem 2. A straight-forward design criterion for the measurement combination would then be to demand that the real part of the fastest unstable pole is at least a certain number ϵ greater than the real part of the closest zero;

$$\text{Re}(p_i) - \text{Re}(z_i) \geq \epsilon, \tag{3.15}$$

where p_i is the fastest unstable pole and z_i is the zero closest to this pole, and ϵ is a fixed positive number. Note that the zero in consideration is the "worst" zero, meaning that no zeros are allowed to the right of this zero in the complex plane.

Now we want to develop some guiding lines for testing whether a given linear combination satisfies the criterion in equation (3.15). We already have the necessary criterion for all zeros to lie in the left half plane (LHP); all coefficients of the polynomial equation must have the same sign. In order to utilize this here, we must make a coordinate transformation; shift the coordinate system along the real axis such that the fastest pole is located a distance ϵ from the origin. Then the Routh stability criterion can be used to determine if a given linear combination guarantee a minimum distance of ϵ to the fastest unstable pole. If all coefficients of the polynomial equation have the same sign, the Routh array give a sufficient test for the zero locations. Let us state these notions in a theorem.

Theorem 3 (Worst Zero Position Theorem)
Let $\mathbf{y}$ *be the measurement vector with components* $(y_1, y_2, \ldots, y_p)$. *Let* $\mathbf{w} \in \mathbb{R}^p$ *be a weighting vector. Consider the linear combination of measurements* $\xi = \mathbf{w}^T\mathbf{y}$. *Let* ϵ *be a fixed positive number. Then,*

introduce a coordinate transformation along the real axis; $s' = s - \delta$, such that the position of the fastest unstable pole p^* of the system is located at Re$(s') = \epsilon$.

Further, let $\mathcal{P}(s')$ denote the numerator polynomial of the transfer function from a scalar input u to the output ξ in the transformed coordinate system. Then, if the Routh criterion is satisfied for $\mathcal{P}(s')$, the distance between the slowest zero and the fastest unstable pole is at least ϵ.

□

Proof
Let the zeros of the transfer function from u to ξ be given by the solutions λ of a polynomial equation of degree n;

$$\mathcal{P}_n(s) = \sum_{i=0}^{n} a_i s^i = 0,$$

where $a_i \in \mathbb{R} \; \forall \; i \in [0, n]$ and $s \in \mathbb{C}$. Let δ be a given real scalar. Let s' denote the δ-translation of s along the real axis; $s' = s - \delta$. Then we have;

$$\mathcal{P}_n(s') = \mathcal{P}_n(s - \delta) = 0.$$

If λ is a solution of $\mathcal{P}_n(s) = 0$, then $\lambda + \delta$ is a solution of $\mathcal{P}_n(s') = 0$. Further, let δ be such that the point $p*'$ representing the fastest unstable pole in the transformed coordinates has real part ϵ. Then, if all roots of the polynomial equation $\mathcal{P}_n(s')$ have negative real parts, all solutions of $\mathcal{P}_n(s)$ have real parts smaller than the number δ, which is equivalent to the following;

$$Re(\lambda_i) \leq Re(p^*) - \epsilon, \quad \forall \; i \in [0, n]. \tag{3.16}$$

This completes the proof.

□

The Worst Zero Position Theorem gives sufficient conditions for a linear combination not to be limited by RHP zeros, but at the same time it gives sufficient conditions for infeasibility of the linear combination approach. If the system is shifted in coordinates as described in Theorem 3, and the resulting numerator polynomial $\mathcal{P}(s')$ does not have the same sign for all its coefficients, we know that the zero lies to the right of the number $p_i^* - \epsilon$ in the complex plane. This, again, follows from the Descartes rule of signs. In other words, if we use ϵ as a threshold for "practical controllability", we have a test for controllability in Theorem 3.

Linear Combination Control of Example Process

We will now investigate if it is possible to control the example process given in equations (3.3) and (3.4). As mentioned, the system has a pair of complex-conjugate poles at $0.5 \pm 0.87j$. The transfer functions have zeros at 0.25 and 0.17 respectively. When two transfer functions have only one zero each, it is always possible to find a linear combination such that the instability is observable (in the practical sense as mentioned).

When the zeros are in the LHP but close to the imaginary axis, performance is often lost due to input saturation. In order to avoid this, we demand the linear combination transfer function to have its zero at

$s = -1$. In other words, find β such that the transfer function from u to $\xi = y_1 + \beta y_2$ has its zero at $s = -1$. That is, solving the following system;

$$\begin{aligned}(-4s+1) + \beta(-6s+1) &= 0\\ s &= -1,\end{aligned}$$

which yields $\beta = -5/7$. In summary, we may decide to control the variable $\xi = y_1 - (5/7)y_2$ which has the transfer function

$$G_\xi = \frac{\xi}{u} = G_1 + \beta G_2 = \frac{\frac{10}{7}(s+1)}{s^2 - s + 1}.$$

Using a proportional controller with gain K_c, we wind up with the closed-loop transfer function from reference r to output ξ;

$$G_{\xi^c} = \frac{(10/7)K_c(s+1)}{s^2 + (\frac{10}{7}K_c - 1)s + \frac{10}{7}K_c + 1}.$$

This is a second order process which can be written on the form

$$\frac{K(s+1)}{\tau^2 s^2 + 2\zeta\tau s + 1} \tag{3.17}$$

with the following parameter values (as functions of controller gain K_c;

$$\tau = \frac{1}{\sqrt{\frac{10}{7}K_c + 1}} \tag{3.18}$$

$$\zeta = \frac{\frac{10}{7}K_c - 1}{2\sqrt{\frac{10}{7}K_c + 1}} \tag{3.19}$$

$$K = \frac{\frac{10}{7}K_c}{\frac{10}{7}K_c + 1} \tag{3.20}$$

A linear second order differential equation has only stable solutions if the damping coefficient ζ is greater than zero. That means, the closed-loop system is stable if and only if

$$\frac{\frac{10}{7}K_c - 1}{2\sqrt{\frac{10}{7}K_c + 1}} > 0,$$

which is equivalent to

$$K_c > \frac{7}{10}.$$

Let us finish the example by designing a stabilizing controller and testing its effect on the original directly measured outputs y_1 and y_2 by simulation.

The main control objective is to keep the process stable. Therefore, we choose a simple design method. Starting with a damping ratio of 0.707 we design a simple proportional controller. Using the expression in equation (3.19) for the damping coefficient, we end of with the following quadratic equation for the gain;

$$\frac{100}{49}K_c^2 - \frac{20 + 40\zeta^2}{7}K_c + 1 - 4\zeta^2 = 0. \tag{3.21}$$

With the given value of ζ, equation (3.21) has solutions $K_c = 2.96$ and $K_c = -0.17$, and because the system is only stable for $K_c > 7/10$, we choose the positive solution. The following figure shows the response of a unit step in the reference signal at $t = 1$ (Figure 3.1).

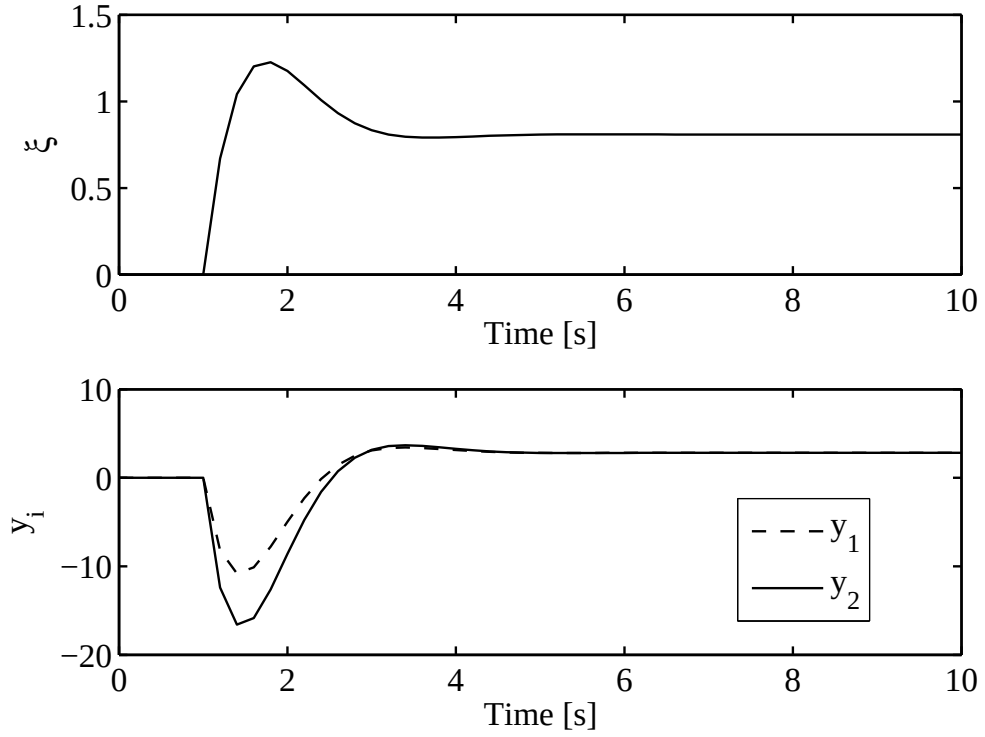

Figure 3.1: Simulation of Linear Combination Control

The controller is efficient in stabilization. Set point tracking is poor due to no integral action. Note the responses in the measurements; the RHP zeros yield inverse responses.

3.3 Case Study: The Storkaas Model

Although the linear combination approach used with the example process was successful in stabilizing the system, the same approach might not be able of stabilizing the real pipeline-riser system due to higher order numerator dynamics. We aim to investigate this by analyzing a linear model obtained by linearization of the Storkaas model.

As mentioned earlier; the two measurements directly available are phase fraction and topside pressure. Using the Storkaas model, we develop transfer functions from the valve opening z to these measurements. The outputs are $y_1 = P_1$, $y_2 = P_2$ and $y_3 = \alpha$. Linearizing around z = 0.25 we obtain the following transfer functions;

$$G_1 = \frac{y_1}{u} = \frac{-0.21s - 0.034}{s^3 + 5.82s^2 - 0.55s + 0.07} \tag{3.22}$$

$$G_2 = \frac{y_2}{u} = \frac{-0.078s^2 + 0.37s - 0.031}{s^3 + 5.82s^2 - 0.55s + 0.07} \tag{3.23}$$

$$G_3 = \frac{y_3}{u} = \frac{11.25s^2 - 0.68s - 0.0072}{s^3 + 5.82s^2 - 0.55s + 0.07}. \tag{3.24}$$

The system's poles are located at $s = -5.91$ and $s = 0.048 \pm 0.095j$. The zeros of the transfer functions are;

G1 $s = -0.1654$; no problem.

G2 $s = 4.65$ and $s = 0.09$; Both zeros are located to the right of the unstable poles in the RHP.

G3 s=0.069 and s = -0.0092; the LHP zero is not a fundamental limitation, but in practice the closeness to the imaginary axis may cause problems with input saturation. The RHP zero is slower than the unstable poles.

Linear Combinations

A natural question that arises here is if it is possible to find a linear combination that is controllable as with the example process. We define the linear combination of measurements as

$$\xi = y_2 + \gamma y_3$$

and demand that γ should be chosen such that all zeros of the transfer function from u to ξ fulfill the condition

$$\text{Re}(z_i) < 0.048 - \epsilon.$$

We choose the "magic line" to lie at $\text{Re}(s) = -1$ as with the example process. Thus, our problem is to find γ such that Theorem 3 is satisfied for $\delta = 1.048$. Expressing the numerator dynamics of ξ as a function of γ we get the following numerator polynomial;

$$\mathcal{P}_2(s;\gamma) = (11.25\gamma - 0.078)s^2 + (-0.68\gamma - 0.37)s - (0.072\gamma + 0.031).$$

Introducing the coordinate transformation by subtracting the real number δ from s, we arrive at;

$$\begin{aligned} \mathcal{P}_2(s';\gamma) = \mathcal{P'}_2(s;\gamma,\delta) &= (11.25\gamma - 0.078)s^2 \\ &+(-22.5\gamma\delta + 1.156\delta - 0.68\gamma + 0.37)s \\ +11.25\gamma\delta^2 - 0.078\delta^2 + 0.68\gamma\delta - 0.37\delta - 0.072\gamma - 0.31. \end{aligned} \tag{3.25}$$

We set as a design criterion $\delta = 1.048$. Inserting this into equation (3.25), we arrive at;

$$\mathcal{P'}_2(s,\gamma,\delta = 1.048) = (11.25\gamma - 0.078)s^2 - (0.68\gamma + 22.52)s + (13.07\gamma - 0.85). \tag{3.26}$$

The task is now to select γ such that all roots of the equation $\mathcal{P'}_2(s,\gamma,\delta = 1.048) = 0$ has negative real parts. A necessary criterion for this, as discussed in the example process case study, is that all coefficients

of the numerator polynomial have equal signs. To check this condition, we set up the following set of inequalities;

$$\begin{aligned} 11.25\gamma - 0.078 > 0 \\ -0.68\gamma - 22.52 > 0 \\ 13.07\gamma - 0.85 > 0 \end{aligned}$$

By solving the second inequality for γ, we see that $\gamma < -33.2$. This is in contradiction with both the other inequalities; hence it is impossible to place the zeros at $\text{Re}(s) = -1$. The problem is so grave, that even flacing the worst zero between the imaginary axis and the fastest unstable is impossible. Therefore; the linear combination approach cannot be used for the problem at hand.

3.4 What Can be Done When Linear Combination Control Fails?

Since we have seen that the linear combination approach is not applicable to the current problem, we must seek other options for topside stabilization. A typical solution used in the process industries to improve performance of bandwidth limited systems is to use cascade control. It has been shown by among others Storkaas (2005) that the volumetric flow rate has no RHP zeros. The problem with the flow dynamics is that the transfer function from z to Q has a very low gain; hence it is not possible to keep the process within the linear range when disturbances occur. In order to remedy this problem, the cascade control approach is to wrap another feedback loop around the flow controller, using the flow controller set point as the controller output. Several cascade configurations for slug repression have been suggested, among them using topside pressure, choke valve pressure drop and the valve opening as measurements for the outer loop. The cascade approach is discussed in the next chapter.

Another possibility is to use a state observer. This approach demands a fairly accurate process model with limited complexity. The latter because the model must be solvable faster than real-time. The observer approach will be discussed in Chapter 5.

Chapter 4

Cascade Control using Topside Measurements

4.1 Introduction

The possibility of using cascade control based on topside measurements only for slug repression has shown fruitful both theoretically Storkaas (2005) and experimentally Godhavn et al. (2005).

Two different schemes are tested here; both with an estimate of Q in the inner loop. This measurement has a very low gain, but no RHP zeros. That indicates it should be possible stabilize the flow using a flow controller, but the low gain causes poor robustness; the process is prone to drift away from the desired operating point.

In order to increase tracking performance, a master loop is wrapped around the flow controller, where the set point for the flow controller is set by the outer controller. Two different schemes are suggested by Storkaas (2005);

- Q in inner loop and P_2 in outer loop
- Q in inner loop and z (valve opening) in outer loop.

The last suggestion is rather exotic, but Storkaas claims a slow resetting of the valve opening to the desired average value is a viable option to avoid drift.

Cascade implementation has been attempted, but the flow rate cannot be directly measured in the laboratory setup. Therefore, the volumetric flow has to be estimated. This has been done using a simple valve equation. The valve equation depends on an estimate of the mixture density, which is obtained using light absorption in the fluid as an indicator of liquid fraction. This measurement is noisy, and therefore the flow rate estimate is hard to obtain in a robust and reliable manner.

Before going to the experimental part, a short review on cascade control will be given.

4.2 Cascade Control Theory

For this section we assume that a reliable measurement of the volumetric flow through the choke valve is available.

The normal cascade control configuration has nested loops; where the slave loop is inside the master loop. Then the inner loop is designed first. The closed-loop system is then regarded as the system we want to control when designing the outer loop. The inner should must be significantly faster then the outer loop, such that we may approximate the dynamics of the inner loop as infinitely fast when designing the outer loop. The cascade structure is shown in Figure 4.1.

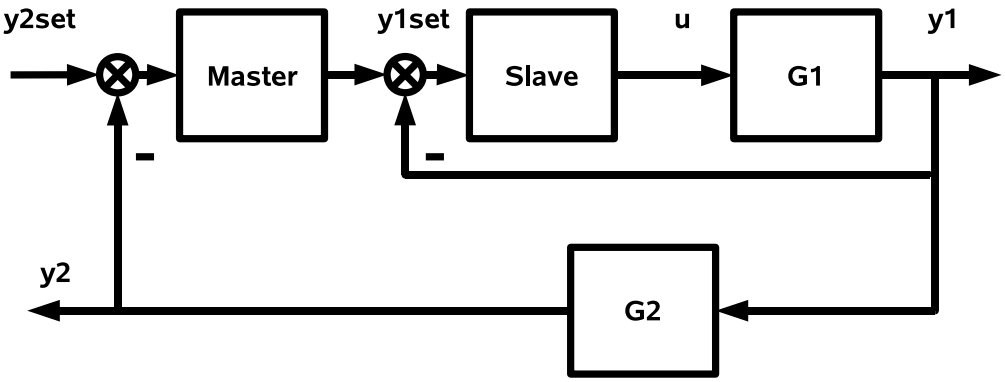

Figure 4.1: Block diagram of cascade control configuration

Cascade control is often used to improve disturbance rejection. Here we use the system for this purpose; the inner loop is there to stabilize the system. The task of the outer loop is to ensure better performance at lower frequencies such that the system does not start to drift, which would cause the instability to reoccur when the state is outside the acceptable range for the flow controller.

Let K_m be the transfer function of the master controller in Figure 4.1 and K_s be the slave controller. The first task in designing the cascade system is to stabilize the inner loop. The closed loop transfer function from Q_{set} to Q is

$$G_{\text{Inner}} = \frac{K_s G_1}{1 + K_s G_1}. \tag{4.1}$$

When approximating the dynamics of the inner loop as infinitely fast, we simply set $Q = Q_{\text{set}}$ when designing the outer loop. This might be an over-simplification, and the correct transfer function from $P_{2,set}$ to P_2 is

$$G_{\text{Cascade}} = \frac{K_M G_{\text{Inner}} G_2}{1 + K_M G_{\text{Inner}} G_2}. \tag{4.2}$$

4.3 Model-Based Analysis

The following analysis is based on a linearization of the Storkaas model around the desired operating point, which is an unstable equilibrium point. We consider the following measurements to be available; total volumetric flow through choke valve, downstream pressure and the valve position itself. The upstream pressure may also be considered in a cascade loop, where flow control is used to increase the speed of response.

A measurement of the gas flow has shown that the air feed to the experimental system has mostly been approximately 9 L/min at STP, and therefore the Storkaas model is linearized again with this change to the

setup. The desired operating point is a "seabed" pressure of 0.2 barg and topside pressure 0.02 barg. These values have shown to be easily obtained experimentally when using feedback with P_1 as the controlled variable. Linearizing around $z = 0.25$ and the given pressures, we obtain the following transfer function model.

$$G_1 = \frac{P_1 \text{ [bar]}}{z} = \frac{-0.88s - 0.21}{s^3 + 16.9s^2 - 3.95s + 1.21} \tag{4.3}$$

$$G_2 = \frac{P_2 \text{ [bar]}}{z} = \frac{-0.18s^2 + 0.78s - 0.19}{s^3 + 16.9s^2 - 3.95s + 1.21} \tag{4.4}$$

$$G_3 = \frac{Q \text{ [L/min]}}{z} = \frac{49.2s^3 + 342s^2 + 72s + 1.62}{s^3 + 16.9s^2 - 3.95s + 1.21} \tag{4.5}$$

Note that a direct measurement of Q is not available in the laboratory, such that this variable has to be estimated. This will be neglected in the following analysis, and the variable is treated as directly measureable.

The general trend is the same as mentioned before; we have a pair of complex conjugate unstable poles, this time located at $s = 0.12 \pm 0.23j$. In addition, we have a stable pole at $s = -17.1$. The upstream pressure has a single zero at $s = -0.24$ and the topside pressure has its two zeros at $s = 0.26$ and 4.01 respectively. Both zeros are here to the right of the unstable poles in the complex plane, and therefore the instability is not observable in this measurement. The steady-state gain of the transfer function from z to P_2 is -0.18. This shows that the variable might be suited for use in the outer loop to gain low-frequency performance of an already stabilized system. The last measurement, volumetric flow, has no zeros in the RHP and can therefore be used to stabilize the flow. On of the zeros is, however, close to the imaginary axis, and this yields poor low-frequency performance; the stabilized system may very well drift out of the linear region. Their zeros are located at $s = -6.714$, $s = -0.20$ and $s = -0.025$.

Controller Design and Simulation

First we design the inner loop using Q as the measurement. Because of zeros close to the imaginary axis, the system is prone to drift when stabilized by flow control. Therefore, a simple proportional controller is used for the stabilization, and the outer loop improves low-frequency performance.

In order to design the controller, some considerations regarding valid ranges for the variables must be made. The valve position is, of course, limited to the range 0 to 1. The system was linearized around $z = 0.25$, which means in the linearized system we may only allow valve openings between $z = -0.25$ and $z = 0.75$. Further, we also need to consider the steady-state value of Q. At steady-state we have $\dot{m}_{L,in} = \dot{m}_{L,out} = 3.5$ kg/min. The water is considered incompressible, and with a density of approximately $1\ kg/L$, we have $Q_{L,out} = 3.5$ L/min. The same relationship must be valid for the air flow (on mass basis), and with an inflow of 9 L/min at STP (corresponding to 10.6 kg/min), we can calculate the volumetric flow rate of the gas through the choke by using the known pressure $P_2 = 0.02$ barg. The ideal gas law yields;

$$\rho^*_{G2} = \frac{P_2 M_w}{RT} = \frac{1.02 \text{ atm} \times 28.9 \text{ g/mol}}{0.08206 \text{ L atm/K mol} \times 298 \text{ K}} = 1.21 \text{ g/L}.$$

That gives $Q^*_G = 8.78$ L/min, and in total we have $Q^* = 12.3$ L/min or in SI units 2.05×10^{-4} m^3/s. On a mass basis we may assume that the variation in flow through the choke valve in a stabilized regime is

not more than $\delta\dot{m} = \pm 0.5$ kg/min, which at the given conditions (the linearization point) corresponds to a volumetric flow variation of

$$\delta Q = \frac{\delta\dot{m}}{\bar{\rho}} = \frac{0.5 \text{ kg/min}}{0.29 \text{ kg/L}} = 1.7 \text{ L/min}.$$

Slave Controller

The task of the inner controller is to yield stabilization by moving the poles into the LHP. Because of two zeros located close to the imaginary axis, the poles cannot be moved far into the LHP. Hence, furher stabilizing effect can be achieved by the outer loop using PI control to eliminate set point offset. Assuming that the inner loop is very fast, we need to design a system that controls P_2 using r_1 as input.

The inner loop is controlled with a pure gain. Setting the gain to $K_c = 1$ we get the following closed-loop characteristic equation;

$$50.2s^3 + 358.9s^2 + 68.05s + 2.83 = 0,$$

with solutions $s = -6.96, s = -0.13, s = -0.061$. Hence, the system is closed-loop stable.

Master Controller

Seen from the Master Controller, the task is to control an open-loop stable system with only real poles and zeros. Then, the first idea is to try SIMC design of a PI controller. The transfer function from r_1 to P_2 is

$$G_{\text{CV}} = \frac{-0.067(s - 4.074)(s - 0.26}{(s + 6.96)(s + 0.13)(s + 0.061)}. \tag{4.6}$$

Using the "half rule" and the SIMC tuning rules by Skogestad and Postlethwaite (2005), we arrive at the following first order approximation to G_{CV};

$$\tilde{G}_{\text{CV}} = \frac{-0.0671e^{-8.1s}}{20.25s + 1}. \tag{4.7}$$

The tuning relations yield;

$$K_c = \frac{1}{k}\frac{\tau}{\tau_c + \theta} = (1/-0.0671) \times \frac{20.25}{8.1 + 8.1} = -18.7$$

and

$$\tau_I = \min\{\tau, 4(\tau_c + \theta)\} = \min\{20.25, 4 \times (8.1 + 8.1)\} = 16.2,$$

where we have used the common choice of the tuning parameter $\tau_c = \theta$. Before testing the tuning with simulations, consider the Bode diagram of the open loop system shown in Figure 4.2. We see that the phase and gain margins are acceptable, and the system behavior can be expected to be good.

The phase margin using the SIMC controller is 43°. The gain margin is 3.45. Seborg et al. (2004) give guidelines for designing PI controllers based on phase margin and gain margin criteria, and claim that a well-tuned controller should generally have a gain margin between 1.7 and 4.0 and a phase margin between 30° and 45°. The SIMC controller is well into this interval, and we may therefore expect the system to be well-behaved, at least within the validity region of the linearization.

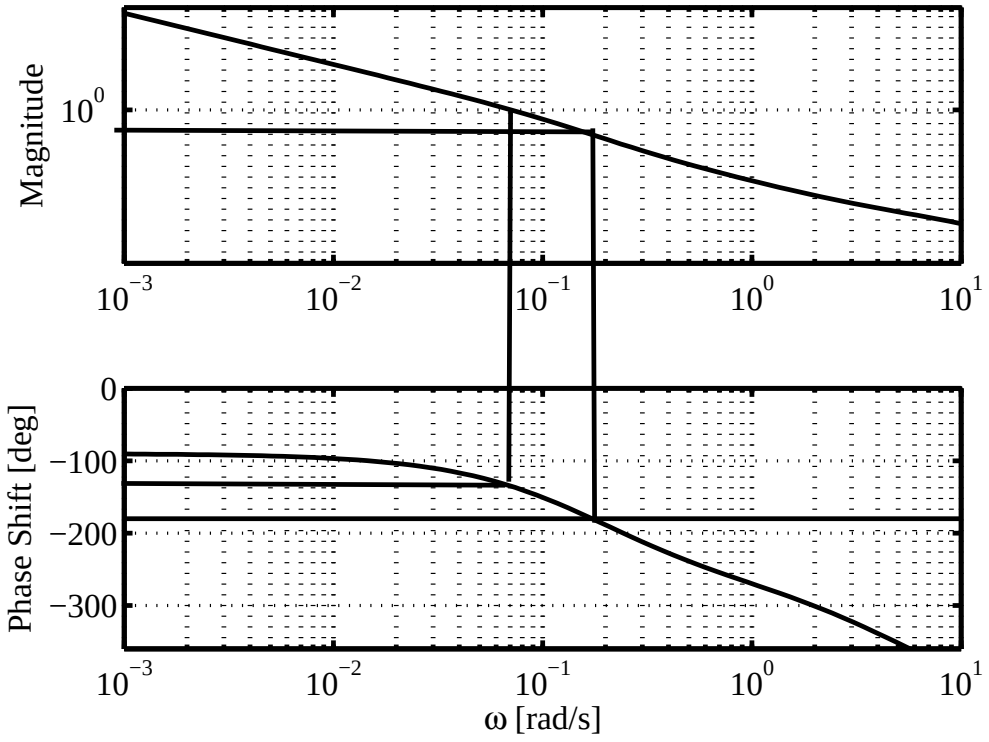

Figure 4.2: Bode plot for open loop transfer function from r_2 to P_2 with SIMC PI controller

Linear Simulation

Let us consider a simulation of the closed-loop system based on the linear model. We assume a set point change in P_2 from 0.02 bar gauge pressure to 0.015 bar at $t = 0$.

The set point tracking is good. The result is shown graphically in Figure 4.3. Note the offset in the inner loop due to the pure gain controller. The P_2 set point tracking, however, is excellent.

Next, consider an output disturbance in the volumetric flow. Assume a disturbance of 0.1 L/min 4 minutes after a set point change. Figure 4.4 shows the result of the disturbance in flow rate and pressures. We observe that the given tuning parameters are not able of stabilizing the plant with good robustness to output disturbances.

As the SIMC controller was not robust enough, trial and error was used for tuning the controller. Using $K_c = -0.5$ and $\tau_I = 2$ we obtained acceptable set point tracking and disturbance rejection, as shown in Figure 4.5.

4.4 Nonlinear Simulation of Cascade Control

Using a linear plant model, we have shown that it should be possible to obtain good anti-slug control using cascade with flow rate in the slave controller and pressure in the outer loop. It is interesting to see how these controllers perform with a more rigorous nonlinear model.

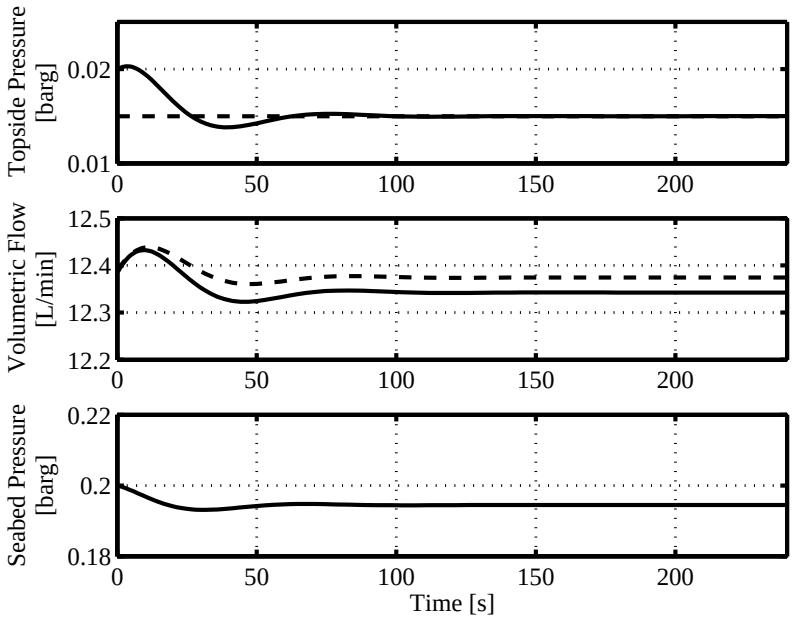

Figure 4.3: Set point tracking is good when using a SIMC controller in the outer loop.

The Storkaas model is used for the simulations. When working with linear models we enjoy the nice behavior of linear systems, most importantly the property of superposition. When working with nonlinear systems, this is no longer so. Therefore, the effect of a disturbance cannot be predicted by simply adding an extra term in the feedback loop.

Controller Design based on Nonlinear Model

The controller settings from the linear analysis were attempted used in a nonlinear model, but the system was not solvable using the available methods in Simulink. Therefore, a new design based on the nonlinear model was attempted.

First, the flow is stabilized by using a proportional controller. The set point for the controller was estimated by stabilizing the system with bottom-side pressure control and looking at the average volumetric flow through the choke. When stabilized to a set point of $P_1 = 0.02$ barg, the flow through the choke is 12.3 L/min, in agreement with the steady-state considerations made for the linear design earlier. The model implemented in the S-function in Simulink operates with standard SI units. 12.3 L/min corresponds to a flow of 2.05×10^{-4} m^3/s. To have convenient numbers, we scale the flow measurement by multiplication with 10000, such that we have an initial set point of $\tilde{Q} = 2.05$.

Now we stabilize the flow using a pure gain of $K_c = 4$ in the feedback loop. Introducing a small step in the controller reference signal makes it possible to identify a simplified first-order plus dead time model in transfer function form from the flow controller reference to the variable chosen for the outer loop. We will

[0]This number has the rather special unit of kL/s (kiloliter per second).

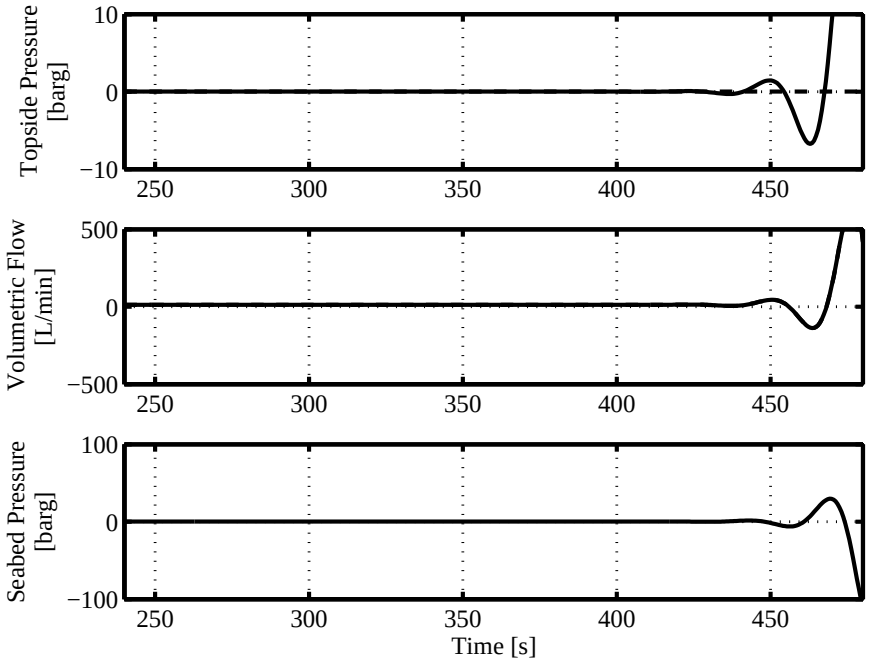

Figure 4.4: Effect of disturbance in flow rate (Q)

consider both using the top-side pressure and the valve position itself.

Model Reduction; Estimating Transfer Function Models from Slave Reference to Master Controlled Variables

We consider for the master loop the variables P_2 and z. Doing one at the time, we start with the pressure measurement.

Master Controlled Variable: P_2
Looking at the step response in P_2, it seems natural that the measurement can be represented well with a first-order linear model for a closed-loop system. The transfer function was estimated to

$$G_{P2} = \frac{-0.43e^{-10s}}{45s+1}. \tag{4.8}$$

Using this transfer function, we get a good fit to the nonlinear model. The maximum residual norm Residual $= P_{2,\text{linear}} - P_{2,\text{nonlinear}}$ is 10^{-3}, which should be good enough for engineering purposes. A graphical representation of the step test is given in Figure 4.6.

Master Controlled Variable: z
Using the same procedure as for the pressure measurement is not very tempting because the measurement

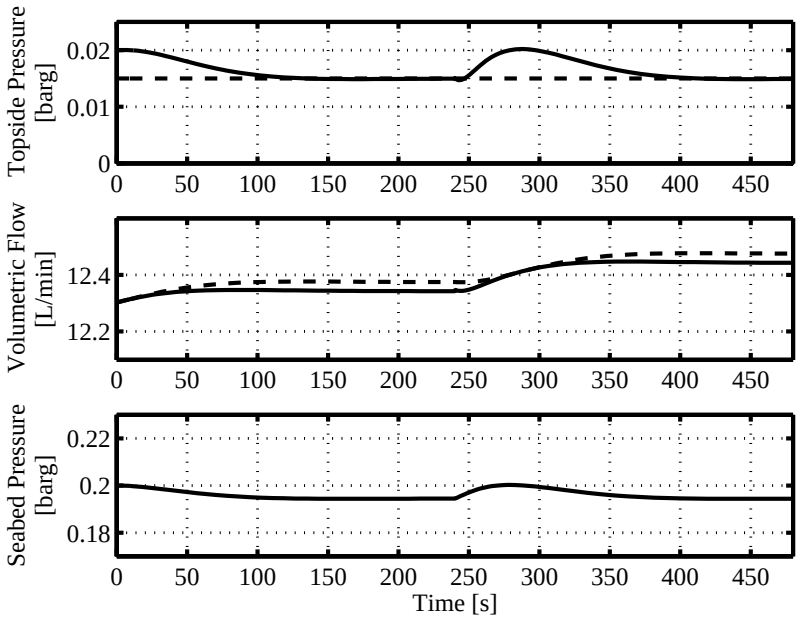

Figure 4.5: Low gain in outer loop; making the master controller slower improves robustness

in consideration is at the same time the manipulated variable of the inner loop. Consider the standard SISO feedback system shown in block diagram form in Figure 4.7.

Assume for a moment that the controller K and the plant G can be described by transfer functions. Then we can express the input-output behavior from r to z as a transfer function;

$$\frac{z}{r} = \frac{K}{1+G}. \tag{4.9}$$

Using a step test in the input again, we can fit a first-order plus dead time model to the response. The fit is not quite as good in the beginning of the response as for the P_2 model, but the maximum residual is 0.011. The residual converges to zero at the new steady-state, that is, the gain is correct. The residual plot is shown in Figure 4.8.

The identified transfer function has a smaller time constant than the one from Q_{set} to P_2, which is the expected behavior; the dynamic path from the reference signal to the controller output is much shorter than from the reference signal to the pressure upstream the valve; in other words, the plant P_2/Q_{set} has higher-order dynamics than z/Q_{set}. The identified transfer function is;

$$G_z = \frac{1.594e^{-10s}}{33s+1}. \tag{4.10}$$

Design of the Master Loop

Now that we have transfer functions for our candidates as master controlled variables we may procede with the master controller design. The slave stabilizes the system, hence we have no poles in the RHP. The

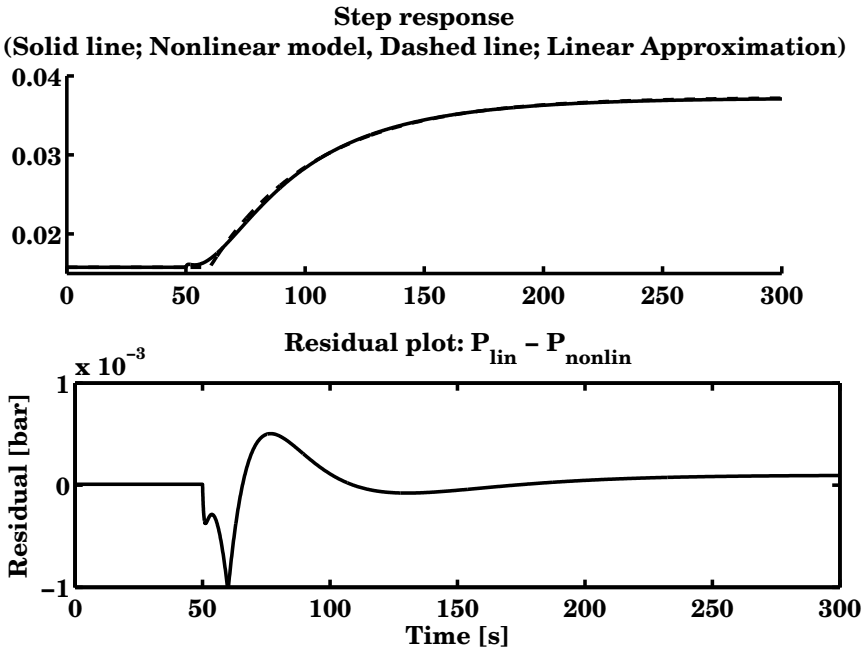

Figure 4.6: The FOPDT model is well able of fitting the nonlinear model's behavior when excited by a step in the reference signal.

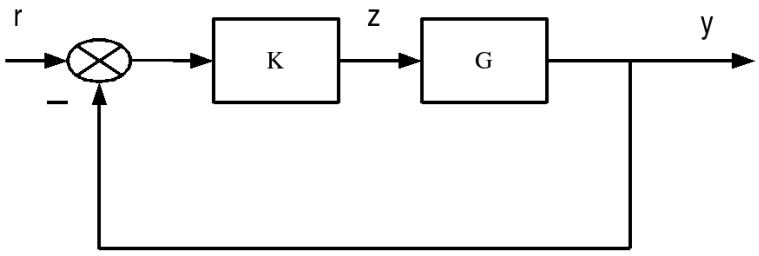

Figure 4.7: Standard SISO negative feedback loop where K is the controller and G is the plant.

identified transfer functions fit the behavior of the nonlinear system well, at least in the frequency range of the step excitation, and the controller for the master loop may therefore be designed using the simple SIMC method Skogestad and Postlethwaite (2005). The SIMC design rules were discussed in Section 4.3. We first design the controllers for both P_2 and z in the outer loop, then we test their effect on the system by simulation.

P_2 in the outer loop

Using the recommendatino by Skogestad for fast and robust control and setting the tuning parameter τ_c of the SIMC rules equal to the dead time θ in the identified first-order model, we get the following results for

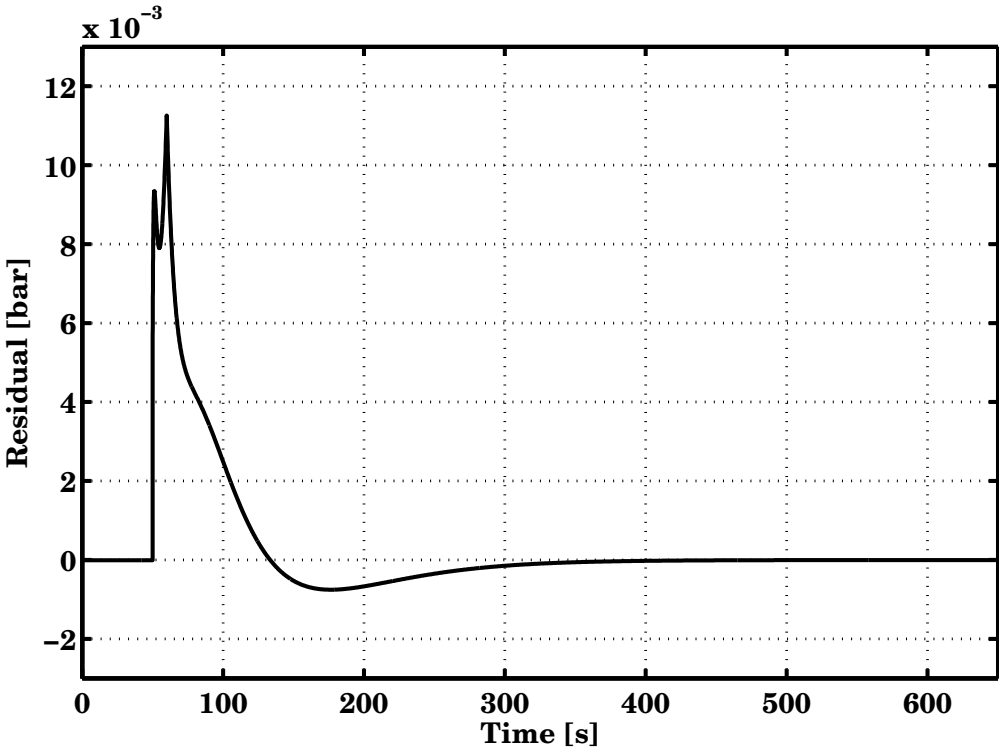

Figure 4.8: Residual plot for identification of transfer function from Q_{set} to z.

the PI controller;

$$K_c = \frac{1}{k}\frac{\tau}{\tau_c + \theta} = \frac{1}{-0.43}\frac{45}{10+10} = -5.23$$
$$\tau_I = \min\{\tau, 4(\tau_c + \theta)\} = \min\{45, 80\} = 45.$$

z in the outer loop
From the identified model we get the following PI settings when using z in the outer loop;

$$K_c = \frac{1}{k}\frac{\tau}{\tau_c + \theta} = \frac{1}{1.594}\frac{33}{10+10} = 1.04$$
$$\tau_I = \min\{\tau, 4(\tau_c + \theta)\} = \min\{33, 80\} = 33.$$

Nonlinear Simulation Study

The tracking ability of the system is tested. First, we look at the control system where P_2 is the primary controlled variable, and we use the PI controller developed above by the SIMC rules. First we allow the system to stabilize at $P_2 = 0.02$ and then introduce a step in the reference from 0.02 to 0.015. The tracking ability of the system seems to be very good. The primary controlled variable and the valve opening are shown in Figure 4.9.

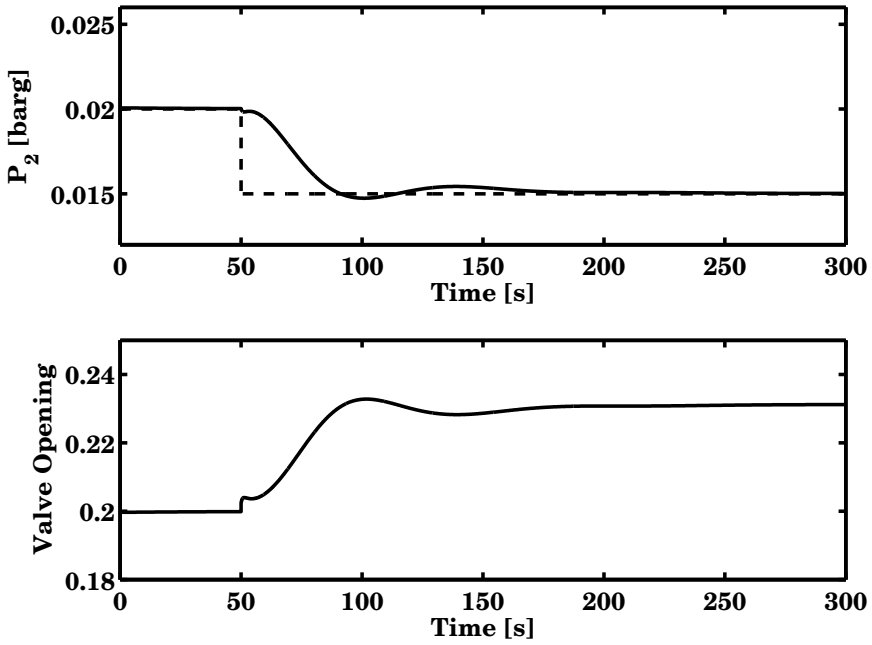

Figure 4.9: Results of nonlinear simulation of cascade control with P_2 in outer loop. The set point is shown as the dashed line in the top plot. We see that the use of the SIMC controller yields tight reference tracking.

Now we turn to the other case, using z as the primary controlled variable and at the same time as output from the slave controller. As test case here, we want to simulate the system around approximately the same state trajectory as in the case with control of P_2 directly, therefore we chose as test signal a step from $z = 0.2$ to 0.24 in the reference signal to the master controller.

The result is remarkable; it is possible to stabilize the system without using a pressure measurement (unless pressure is used to estimate the flow).The performance with regard to a step in the reference signal is comparable to that of the P_2-controlled system. The system response is shown in Figure 4.10.

By comparing to two responses we note that the tracking ability of the P_2 system is slightly better than the z system.

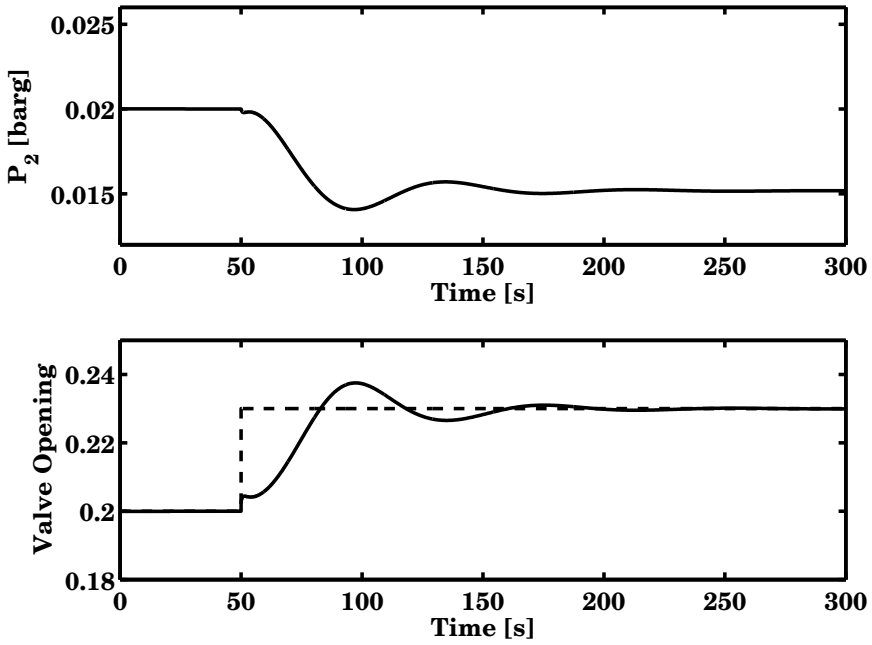

Figure 4.10: Using the valve opening as the primary controlled variable seems a viable option as a substitute for pressure control.

4.5 Remarks on Experimental Work

Experiments with cascade control based on top-side measurements only have been attempted by others, see for instance Baardsen Baardsen (2003). That study showed that stabilization using the available top-side measurements is very difficult. One measurement discussed by Storkaas for use as the controlled variable of the slave loop is the volumetric flow rate of the two-phase mixture. This measurement is used in simulation studies by Storkaas.

A direct measurement of the volumetric flow rate, or the mass flow for that matter, is not available in the laboratory plant. Hence, the flow rate has to be estimated from available data. As discussed by Baardsen, obtaining a good flow estimate is difficult. A simple valve equation based on a Bernoulli-like model of the flow has been suggested;

$$Q \approx K(z) \times z\sqrt{\Delta P/\rho}, \tag{4.11}$$

where the $K(z)$ function is a function depending on the valve opening used to correct for neglected frictional losses. The ΔP quantity is the pressure drop over the valve and the density ρ is the density of the two-phase mixture. The available measurements are the pressure upstream the choke valve, a light absorption measurement used to estimate the phase distribution of the flow. The valve opening is not measured, but the valve dynamics are assumed to be much faster than anything else in the system, such that the signal sent to the valve is treated directly as the actual valve opening.

As we have to make the most out of the available information, a valve equation based on those measurements is suggested. Experiments have shown that the friction correction (the valve constant) is not only a function of the valve opening, but also of the pressure upstream the valve. The functional dependency is

clearly nonlinear in both variables, such that the task of obtaining a reliable flow estimate from the available measurements is indeed a challenge.

In the following, we first develop a valve equation by nonlinear regression. Then the implementation of the cascade controller is discussed and experimental results are presented.

4.6 Two-phase Flow Estimation from a Valve Equation

Flow is to be estimated using a valve equation and measurements of phase distribution and pressure (or pressure drop over the valve). The equation used for this has the following form (inspired by Bernoulli);

$$Q = f(z, P)z\sqrt{\frac{P}{\rho}}, \tag{4.12}$$

where the function $f(z, P)$ is some function of valve opening and pressure describing all irreversible elements of the flow (friction, entropy production).

If we calculate the value of K for different measurements of pure water flow;

$$K(z, P) = \frac{Q}{z\sqrt{P}} \tag{4.13}$$

we can plot the values of K against P for different valve openings. This is done in Figure 4.11. Observe the different behavior with regard to z at valve openings below and above 20%.

Looking at the low-opening data first, we observe that the shape of the data seems to resemble that of a first-order process step response, but where the "gains" and the "time constants" vary with valve opening.

The data for high valve opening also exhibit this negative exponential behavior, and can probably also be approximated by a lag-equation.

Curve Fitting

Low Valve Opening

We first try to fit an equation to the low-opening data. This was done in a very crude fashion by plotting the data on paper and using a pencil and a ruler to "construct" first-order step response graphs. By forcing all graphs to cross the K axis at $K = 53$, and using the initial tangent method to estimate the time constant, we arrived at the following parameters (4.1).

z	K_c	τ
0.10	30	0.090
0.15	38.5	0.081
0.17	47.5	0.068

Table 4.1: Parameter values to estimate K-value in valve equation for valve openings below 20%.

The suggested equation is;

$$K(z, P_2|z < 0.2) = K_0 + K_c(z)(1 - e^{-P/\tau}). \tag{4.14}$$

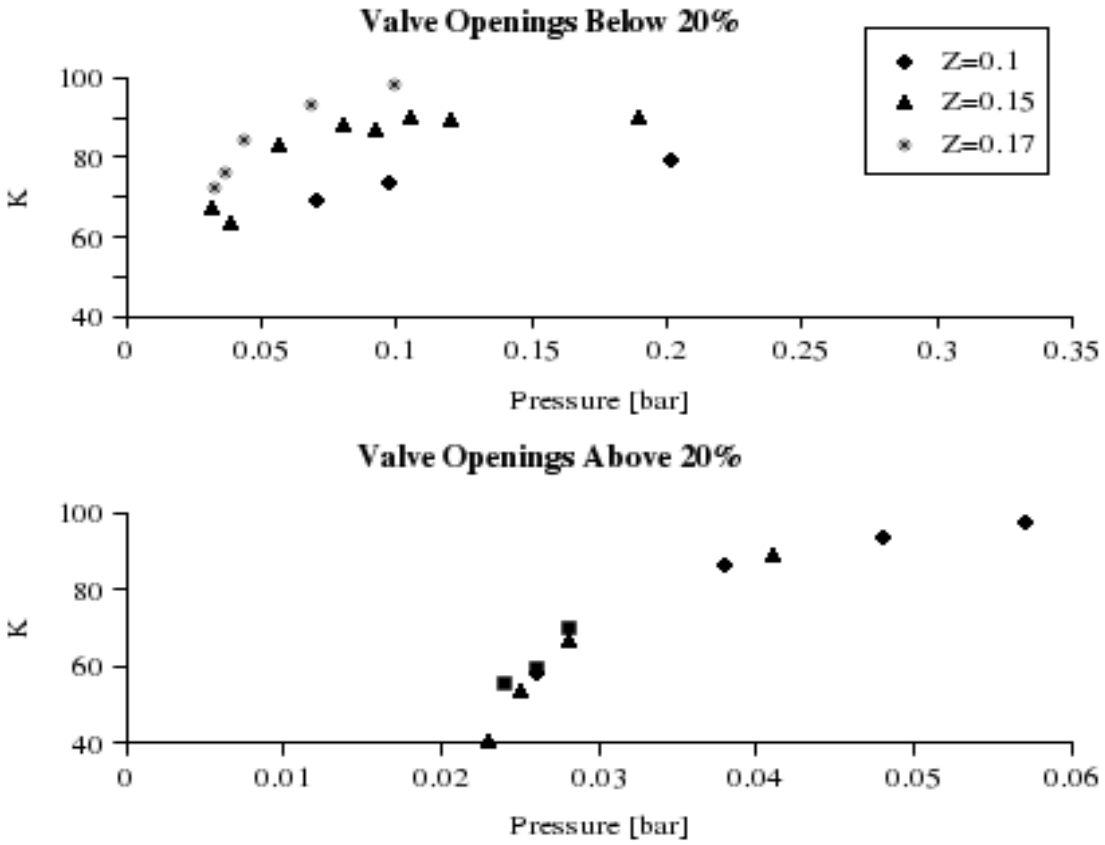

Figure 4.11: Raw data: At low valve openings, the K value is a function of both z and P, but at higher valve openings the dependency of z vanishes.

The data in Table 4.1 are used to fit the K_c and τ dependencies on z to quadratic equations;

$$K_c = 4000z^2 - 830z + 73 \tag{4.15}$$

$$\tau = -1.41z^2 + 0.04s + 0.07. \tag{4.16}$$

Using equation (4.14), we get the following fit to experimental data (Fig. 4.12).

As we can see from the Figure, the fit is good for the given data. The next step will be to model the K values at higher valve openings, and then testing the equations as flow estimators. Lastly, the estimator will be implemented in a laboratory data logging system and tested in real-time against measured flow rates for pure water.

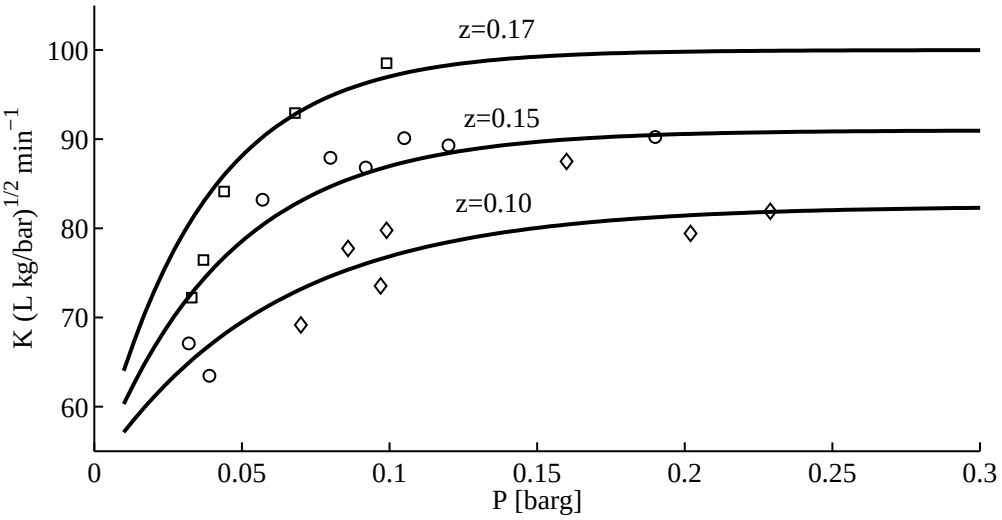

Figure 4.12: Testing the K-value equation

High Valve Opening

As seen from Fig. 4.11, the variation of the data above $z = 20\%$ is much smaller than the low-opening data. The following equation is suggested;

$$K = 14 + K_1(z)(1 - e^{-(P-0.02)/0.0075}) \tag{4.17}$$

The $K_1(z)$ function was found by fitting a quadratic equation to the data;

$$K_1 = -150z^2 + 63z + 79. \tag{4.18}$$

Figure 4.13 shows experimental data and lines predicted by equation (4.17).

Summary

The following valve equation is suggested based on nonlinear regression;

If z < 0.2;

$$Q = [52.5 + (4000z^2 - 830z + 73)(1 - e^{-P/(-1.41z^2+0.04s+0.07)})]z\sqrt{\frac{P}{\rho}}$$

If z > 0.2;

$$Q = [13 + (-150z^2 + 63z + 79)(1 - e^{-P/0.0075})]z\sqrt{\frac{P}{\rho}}. \tag{4.19}$$

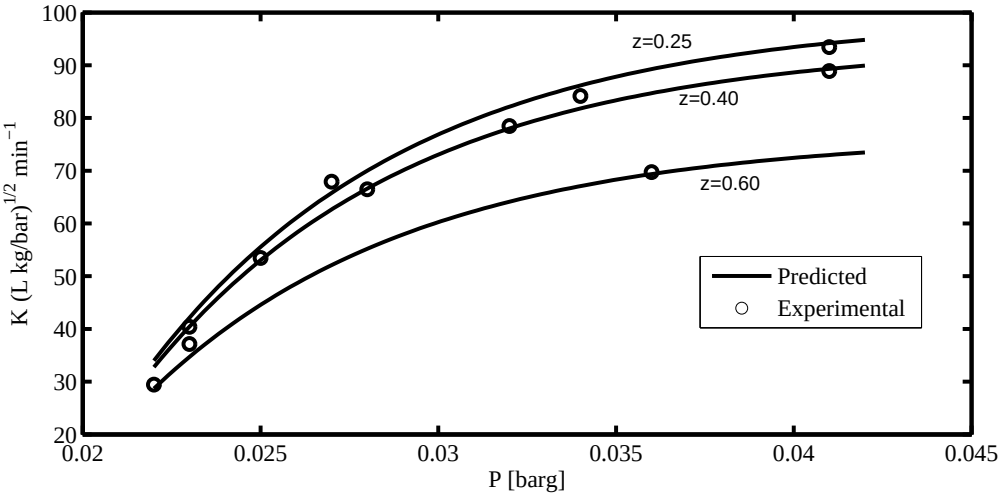

Figure 4.13: Experimental data and predicted values

4.7 Controller Implementation and Testing

The controller was built in LabVIEW. The LabVIEW block diagram is reproduced in appendix A. Here, only a short description of the workings of the cascade controller is given. A flow estimate using equation (4.19) is used as the controlled variable for the slave loop. The controller in the inner loop is a simple proportional feedback controller. The setpoint for the slave controller is set by a master controller. The primary controlled variable is the pressure just upstream the choke valve (P_2). The controller in the master loop is a PI controller with a simple anti-reset windup scheme; the integrand is set to zero whenever the output saturates.

The controller was well able of stabilizing the flow at an average valve opening of about 19% after tuning. This is well into the unstable region as can be seen from the bifurcation diagram in Figure 1.4. A remarkable effect seen from the experimental data is that the topside-control achieves a lower bottom-side pressure at the same average valve opening than does the bottom-side pressure control.The bottom-side pressure when the system was stabilized by the cascade controller is shown in Figure 4.14.

Note how the well-known severe slugging behavior reoccurs shortly after the controller was turned off at t=19 minutes. Let us also consider the behavior of the measurements used in the controller. First, take a look at the estimate of volumetric flow in Figure 4.15. Note also here the amplitude increase when the controller is turned off.

The set point for the flow was calculated by the master controller. The gain of the master controller was low, such that the set point did not change much, it varied between 13 and 16 L/min. We see that there is some offset from the set point; the average value of the estimated flow is slightly higher than the set point range calculated by the master controller.

The primary controlled variable was P_2 as discussed. The upstream pressure did of course oscillate as well as the other measurements, and also here the automatic to manual switch is distinctly visible on the data chart shown in Figure 4.16.

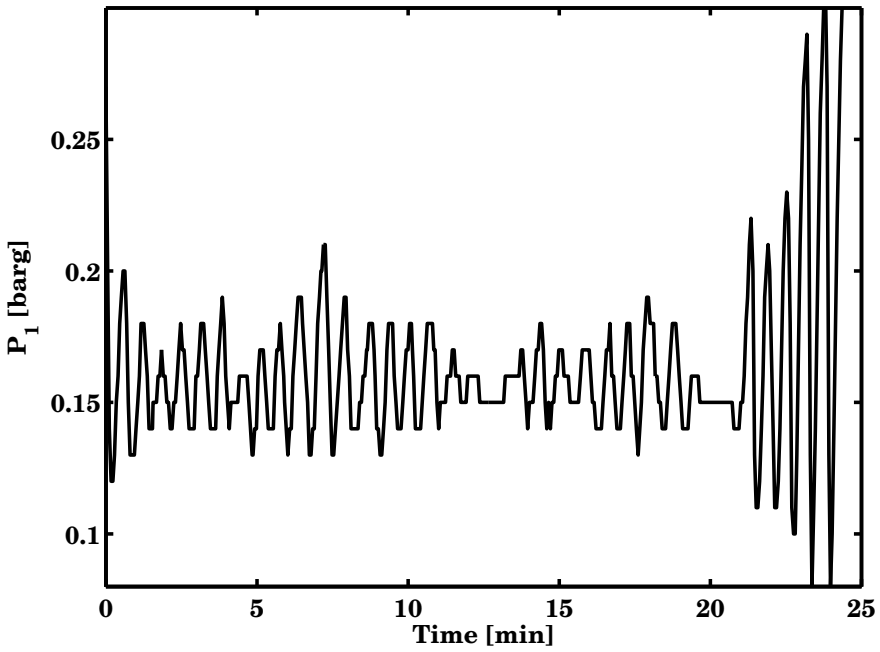

Figure 4.14: Bottom-side pressure under stabilizing feedback control using top-side measurements only.

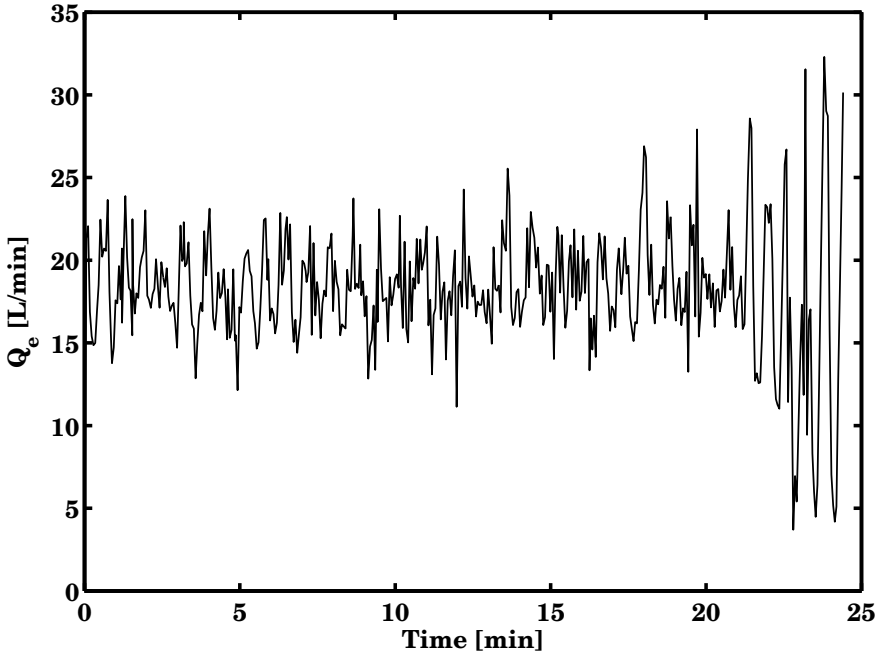

Figure 4.15: The secondary controlled variable; Estimate of volumetric flow rate based on equation (4.19).

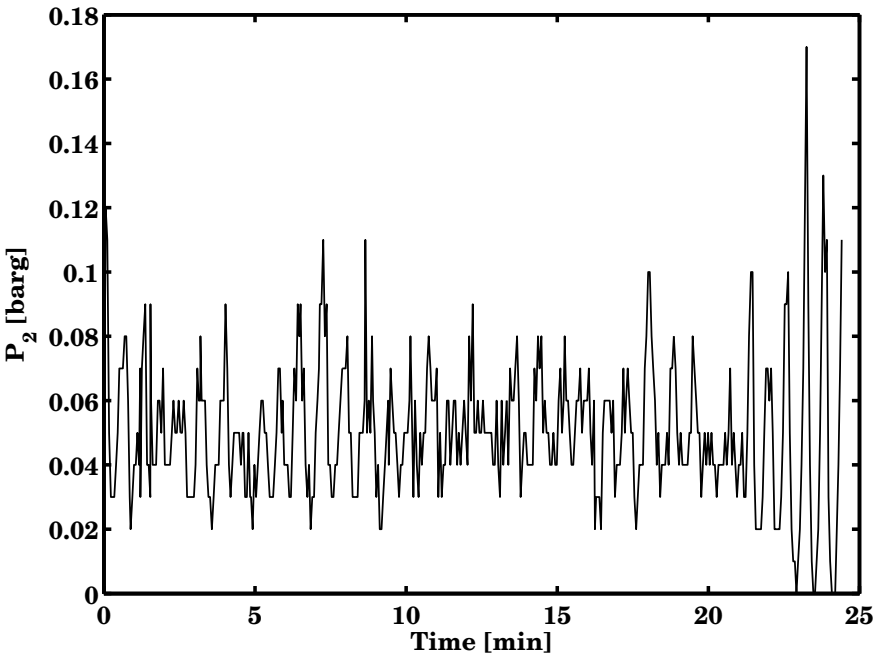

Figure 4.16: Primary controlled variable; top-side pressure (set point $P_2 = 0.05$).

Tuning and Operator Action

The tuning used in the cascade experiment was a gain of $K_c = 0.35$ for the slave controller and $K_c = -0.55$ for the master controller. The integral time of the master controller was $\tau_I = 100$ seconds.

By visual observation it was clear that the stabilized regime was much smoother than the severe slugging of the open-loop system. Further experiments have shown that it is possible to obtain a lower operating pressure of the pipeline when using topside control instead of seabed pressure. The problem with the cascade system is twofold; firstly, the tuning of the controllers is not easy due to ill-posedness of the system. As discussed in the theoretical part of this chapter, when linearizing the Storkaas model it is apparent that the volumetric flow has two poles fairly close to the imaginary axis, and these seriously limits the low-frequency performance of the flow controller. Therefore, first tuning the flow controller and thereafter to use standard methods for tuning PI controllers for stable systems on the open loop is not easily done. The controller tunings described above were found by trial and error.

Another effect of the fact that the flow measurement is prone to drift out of the linear region makes the switch from manual to automatic control hard if the system is initially at severe slugging condition. A fruitful strategy was to put the system in automatic mode and use the gain of the master controller to help the system into a state where flow control is effective. That means, some extra attention from operators is necessary to force the system into the bandwidth of the inner loop. Here we understand by bandwidth the range of frequencies where control is effective, as described by Skogestad and Postlethwaite Skogestad and Postlethwaite (2005) [1].

[1]The bandwidth has a lower limit because of zeros close to the imaginary axis; this makes tight control impossible as can be verified by linear simulations.

Further experimental results are shown in Appendix C.

4.8 Ideas for Improvement of Cascade Control System

Gain Scheduling

A possible solution to the switching problem may be to introduce a gain scheduling scheme to help the system into the correct state.As described above, operator action can help the system into a state such that the flow controller is efficient. It was found by trial and error that a low gain should be used in the outer loop when the flow rate is high and a high gain when the flow rate is low [2]. This increases the response speed of the controller. A division of the gain into three different regions can be foreseen, as depicted in Figure 4.17.

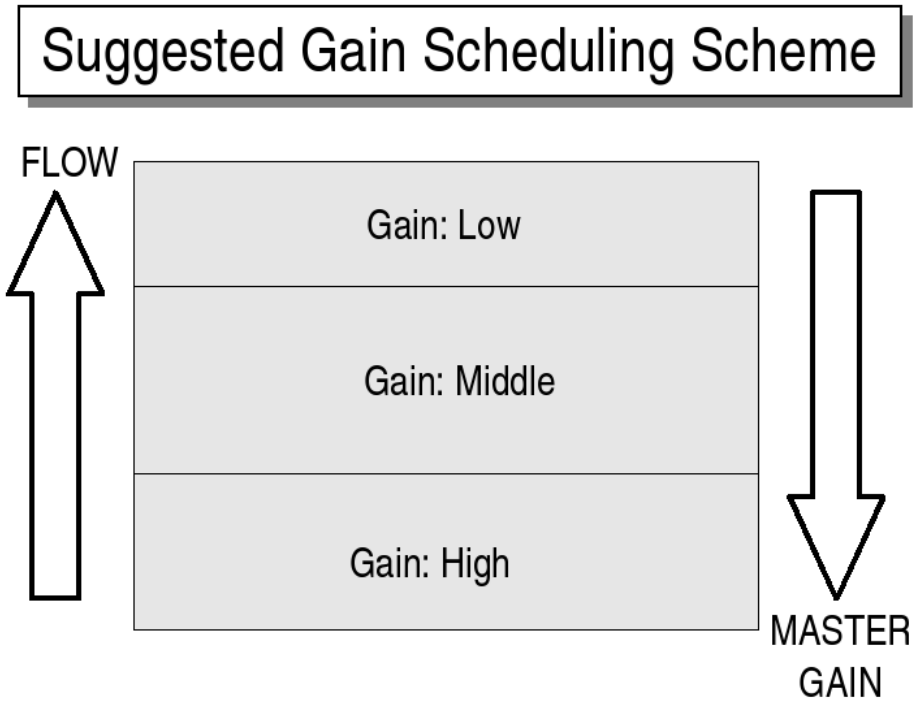

Figure 4.17: The gain of the master controller is increased when the flow is decreased and vice versa.

The gain scheduling scheme will have to be tested experimentally, because the Storkaas model does not model hydrodynamic slugging (small pressure oscillations), and this phenomenon makes controlling the real system harder than than controlling the model system in simulations. An experiment with gain scheduling and topside flow control (not cascade) was done, and the results suggest that this may be a possibility for improving performance of the cascade system. For the experimental data, see Appendix C.

[2] High and low refer to the absolute value; we call K = - 100 a larger gain than K = - 1.

Extra Measurements

We have seen in terms of linear combinations that the use of extra measurements may yield improved control. When using cascade control, one utilizes two measurements directly. In our case these were Q and P_2. The third available measurement is the valve opening. It may be speculated whether a linear combination of z and P_2 in the outer loop can lead to better performance than the use of either one of them alone. This question may be addressed through nonlinear simulation with the Storkaas model.

Chapter 5

Other Possible Control Configurations

5.1 Control Based on State-Observers

The system is state-observable, and a state observer should be a viable option of avoiding problems with top-side measurements. The main problem in developing such an observer is the complexity of the available model. A linear observer could also be an option, a linear model is well able to represent the dynamics around the stabilized operation point, but a linear model cannot model a limit cycle.

Basing control on a linear observer, i.e. a Kalman filter, would probably be a possible solution, but the controller might not be able of stabilizing a system which is already slugging.

In order to solve this problem several strategies can be foreseen;

- start by choking the system into stability, then turn the controller on
- use a nonlinear controller which is able of representing the limit cycle as well as the stabilized equilibrium solution
- use a direct measurement of flow rate to first stabilize the process.

The choking option is maybe the simplest way to use the linear observer. As discussed by citep-storkaas:antislug the unstable equilibrium solution which exists after the bifurcation point is a continous extension of the steady-state regime below the bifurcation point. Therefore, it should be possible to improve this approach considerably by making a piecewise affine model by linearizing around different operating points along the equilibrium trajectory.

The nonlinear observer is maybe the most important solution, as it would be a solution possible to use in the whole operating range. A nonlinear model is available in the Storkaas model, but designing an observer based on this model is problematic due to several reasons. First of all, the model is in implicit DAE form, and is numerically hard to solve. This makes it hard to solve the problem faster than real-time, which makes the model unfit for implementation in a control system. Another problem is theoretical; due to several hard nonlinearities it would be hard to prove stability of the observer, at least globally.

5.2 On/off Control and Gain Scheduling

The non-minimum phase behavior of the topside measurement dynamics cause problems with a controller that reacts to late; the control valve closes too late because the instability is not observable from the available measurements.

Due to this, the following "gain scheduling" approach was tested; The flow estimate is controlled using a P controller; $u(t) = u_0 + K_c e(t)$. The bias is varied by an outer loop in a bang-bang control manner, i.e.;

- if water flows through the valve, set $u_0 = 0.7$,
- else, set $u_0 = 0.2$.

The experimental results are reproduced in Appendix C. The attempt showed some potential for the gain scheduling approach, but the simple system outlined here was not successful in stabilizing the flow.

5.3 Partial Gas Lift

This section is only the outline of an idea, and to assess the feasibility of such an approach simulations based on a more rigorous flow model should be used, for instance OLGA.

The problem with two-phase flow in pipeline-riser systems occurs when the pressure drop over the riser is not large enough to counteract the forces of gravity. Using the choke valve as the only input adjusts the flow resistance in order to stabilize the plant. The system is grossly underactuated as we have at least 3 states we want to control and only one input. The situation would be improved if we could add an extra input with a relatively large gain.

One way of stopping the slugs from staying in the riser is to increase pressure and gas flow at the bottom by pumping gas down to the base of the riser; a gas lift solution. This would change the composition of the flow and hence the flow regime. This wonderful effect comes at a relatively high energy cost.

With partial gas lift, the idea is to inject the gas higher up in the riser, but low enough to penetrate some of the fluid. When the gas and liquid flows from the reservior to the pipeline are relatively constant, there is a critical height for the fluid in the riser, where the liquid level stops when the upstream pressure is not high enough to drive the flow through the riser.

By injecting gas through nozzles at different positions along the riser the average density of the liquid in the riser would decrease, and therefore also the hydrostatic pressure. That would make flow occur at a lower base pressure than earlier. Figure 5.1 shows a schematic of the suggested design change.

Several control applications of the partial gas lift can be imagined but the most obvious is; when the liquid fraction in the top section of the riser dies out, more gas is pumped into the riser at a lower point to dillute the slug and make the bottom pressure able of forcing the liquid out of the riser, and thereby avoiding excessive pressure buildup in the pipeline.

However, the system will have to be tested with simulations, and for this a more detailed model is needed than the Storkaas model, because we want to change the flow properties, which cannot be described by a simple lumped model.

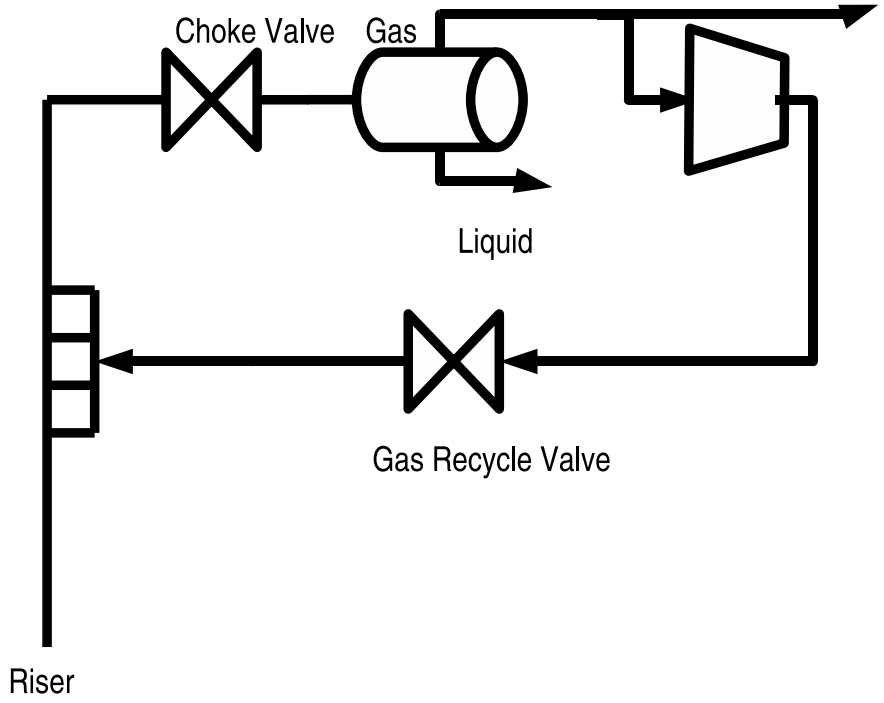

Figure 5.1: Partial gas lift: A fraction of the gas is compressed after the separator and returned to the riser between the base and the top.

Chapter 6

Discussion

This work started with a short introduction to pipeline-riser systems and modeling for applications in control, followed by a description of the experimental facilities. The study was divided in three main parts; one for experimental verification and simulation of feedback control using bottom-side pressure measurements, one part for control using top-side measurements only and a section on controllability and performance using top-side measurements only. A large part of the work consisted of implementation issues for the laboratory mini-plant. The following discussion looks at each topic independently, with a unifying section at the end.

6.1 Implementation Issues for Laboratory Experiments

As mentioned in the experimental part and in Appendix A, the control system and data logging was done using the software LabVIEW from National Instruments Inc. LabVIEW has a built-in graphical programming environment with focuses on signal flow. The development of a control system in LabVIEW is very similar to block diagram constructions in classical control theory, hence the implementation of controllers in LabVIEW is a rapid process.

It was found that the use of LabVIEW for system design was convenient when implementing single components like a controller or process data charts for the operator, but the maintenance of such a system is cumbersome because the block diagram tends to become very cluttered.

The reuse of code is, however, not impractical, because collections of LabVIEW blocks can be collected in a sub VI [1], which corresponds to an external function or method in a traditional programming language. Several sub VI's have been created as a part of this work, and they are documented in Appendix A.

6.2 Bottom-side PI Control

Chapter 2 discusses the use of a PI controller for stabilization and shows experimental results verifying the feasibility of slug repression using feedback. This is only a confirmation of earlier work and current offshore applications. I found it surprisingly easy to obtain acceptable performance using a simple proportional controller.

[1] VI stands for "Virtual Instrument" and is the term used for a LabVIEW program or module.

When comparing experimental results with computer simulations based on the simple Storkaas model, it is clear that the general characteristics of severe slugging are well represented by the model, but the actual properties of the two-phase flow are not well represented; the hydrodynamic (small) slugs which occur around the set point of the stabilized flow are not represented in the model. This is however not necessary for controller design when the design objective is to suppress the large slugs. It does, however, pose a problem when the model is being used for controller performance analysis; the small slugs lead to excessive controller output usage when the gain is high. This is not detectable from simulations based on the Storkaas model.

A PI cotroller is designed based on linearization of the Storkaas model around the desired closed-loop operating point. The design is based on bounds on the bandwidth and sensitivity function, and the behavior of the system seems to be nice when looking at a linear simulation. A nonlinear simulation using the Storkaas model from which the linear model was obtained does however show a different picture, compare Figures 2.3 and 2.4. This indicates that the region around the linearization point where the linear model can be assumed good is smaller than allowed for a set point change of magnitude 0.02 bar for the controller. In other words; if large deviations occur and the controller output changes markably, the linear process model is not a good representation. We also observe that increasing the gain, one manages to keep the process stable in the nonlinear case as well.

Another important thing to note is that the model tuning used for the simulations in Chapter 2 is not very good; the average valve opening of the system as shown in Figure 2.5 is far larger than what is possible to stabilize in practice. This is also commented in Chapter 2.

6.3 Controllability of Non-Minimum Phase Systems

Chapter 3 discusses the controllability of linear non-minimum phase systems. Especially, limitations due to right-half plane zeros are discussed. Background theory on performance limitations is reviewed and an approach to work around the performance limitations using linear combinations of the available measurements is developed.

The linear combination approach has been discussed in connection with self-optimizing control (Skogestad and Postlethwaite, 2005). The use of linear combinations here is meant to make performance limitations less severe by reducing the effect of right half plane zeros. A Theorem based on the principle of superposition for linear systems and the Routh-Hurwitz theorem is developed and proved to evaluate the feasibility of using linear combinations for performance improvements (the "Worst Zero Position Theorem, given as Theorem 3 in Chapter 3). The theorem gives sufficient conditions for infeasibility of the linear combination approach.

Two case studies are done, one on a "Toy Example" meant to illustrate the characteristics of right half plane zeros, and one on a linearized model developed from the Storkaas nonlinear model for slug flow. The result of the Toy Example was that the linear combination approach may drastically improve performance, but tracking control is difficult using SISO control because we are not controlling the actual physical quantities. This may be improved by wrapping another loop outside the linear combination loop, or with the aid of a steady-state process model. Assume we have a system with one input, 3 states and 2 outputs. Let the linear combination be given by $\xi = w^T y$, where w^T is a fixed weighting vector. Let the linear system have state-space realization (A,B,C). At steady state we have;

$$x = -A^{-1}Bu, \tag{6.1}$$

and inserting this into the measurement equation $y = Cx$ we see that the output is uniquely determined by the steady-state value of the system input;

$$y = Cx = -CA^{-1}Bu \tag{6.2}$$

Since the output is uniquely determined, the linear combination is uniquely determined as well, as we see by inserting the fixed weighting vector w;

$$\xi = w^T y = -\underbrace{w^T CA^{-1}B}_{\text{Scalar constant}} u. \tag{6.3}$$

Therefore, a table of corresponding values at steady-state can be set up for use by the operators.

The arguments above do of course only hold for processes where the linear combination approach is able of making the system observable. The other case study, the Storkaas model, was for a more complicated plant with multiple zeros. It was shown that this plant was not controllable using the linear combination approach, at least for the directly measurable outputs.

6.4 Cascade Control Based on Top-Side Measurements

Chapter 4 discussed the possibility of using two top-side measurements in a cascade control system to stabilize the plant. A flow controller has been suggested by others (Storkaas, 2005) for use in the inner loop of the cascade system because the flow measurement does not have any right half plane zeros. The problem with the flow measurement is still in the numerator dynamics; zeros close to the imaginary axis makes low-frequency performance impossible. The practical implication is that it may be possible to stabilize the system using flow control in a feedback loop, but the system will drift away from the set point and most likely become unstable again.

Godhavn et al. (2005) have done experimental work on cascade control earlier. For experiments with flow control, they concluded that finding a good set point was very difficult. This is in agreement with the controllability arguments; the region in state-space where flow control is effective is relatively small.

For simulation studies, a cascade control system was designed on basis of the Storkaas model. The model was re-linearized around a desired operating point and the inner loop was simply set to be a proportional controller. For the linear case, this led to good stabilization.

To obtain acceptable tracking performance and to keep the process in the linear region a master controller was designed, once with top-side pressure P_2 as the controlled variable and once with valve opening z. Both approaches seem interesting from the simulation results; their performances are comparable. This is very interesting because the valve opening is used as output from the controller in the inner loop. In effect, this reduces the number of measurements in the loop. Unfortunately, this option has not yet been investigated experimentally, and because of the crude model experiments are necessary to conclude whether this is a viable option for real pipeline-riser systems.

The controllers for the master loop were designed using the simple SIMC rules. This could be done because the flow controller was able of stabilizing the plant. First-order plus dead time approximations to step responses were identified from numerical experiments with the nonlinear Storkaas model. The model fit seemed very good, and the designed controllers performed very well.

Experiments have shown that stabilization is possible using cascade control using only top-side measurements. The system is however hard to stabilize and to force the system from the slugging condition into

a steady flow regime requires some extra attention from the operator. Some ideas to improve this situation have been suggested, but further work needs to be done in order to check the feasibility of the discussed approaches.

Because stabilization of the flow was obtained by manually adjusting the gain for the outer loop such that the valve opened more at high pressure/flow and back to a smaller valve opening when the slug passed through, the use of gain scheduling seems like a way to automate the operator action.

6.5 Summary

This work has touched a lot of ideas regarding stabilization of severe slugging. We have shown that the use of top-side measurements to stabilize the flow is indeed possible, but also that further work is needed on this. Other possible approaches have been mentioned, both more advanced control strategies including state-observers and design changes. It is, however, more interesting to use cascade control if the solution proves robust enough. There are several good arguments for this;

- the system is easy and cheap to install,
- easy to understand for operators,
- standard controllers and algorithms can be used.

When it comes to robustness, however, the bottom-side solution is probably better. Stabilization using bottom-side pressure as the controlled variable is easy and robust. The downside is that it requires equipment to be placed at the seabed level, which in some cases is hard to do, or the environment at large depths can be very hard on the equipment.

The use of top-side measurements and cascade control can be imagined also for systems where bottom-side measurements are available. First of all, the dynamics for choke valve opening to a flow measurement are much faster than the pressure dynamics. Therefore, when large transport delays are acting a system using top-side flow and bottom-side pressure can also be foreseen. Another point is that the top-side cascade system can be used as a backup in case of fallout of the bottom-side measurement.

Appendix A

LabVIEW and MATLAB Source Code and Comments

This appendix gives a short overview of code developed as a part of this work. The software is internally documented and this appendix only serves to present the main ideas and workings.

LabVIEW Components

As described in the main part, controller implementation and data logging was done with LabVIEW. LabVIEW is a program developed and marketed by National Instruments Inc. The VI's shown here are developed and tested with LabVIEW Professional 8.0. There are several available versions of LabVIEW, including different sets of components. Therefore, if one is using another version than the one mentioned here, all pre-made libraries may not be available. For details, see the web site of National Instruments (*http://www.ni.com*).

The hardware used for the experimental work was also delivered by National Instruments, and a convenient interface between the hardware and the computer comes "out of the box". For other solutions the hardware follows the RS-232 electronic interface standard (IEEE).

PI Controller With Anti-Reset Windup

The PI controller has been described in the text. The anti-reset windup mechanism is very simple. The PI controller has the following control algorithm in the time domain;

$$u(t) = K_c \left(e(t) + \frac{1}{\tau_I} \int_0^t e(\tau) d\tau \right). \tag{A.1}$$

The anti-reset windup scheme simply sets the integrand ($e(\tau)$) to zero if the output saturates. In LabVIEW block diagram form, the algorithm is shown in Figure A.1. The blocks are not so easy to see on a small figure, the picture is included simply to show how programming is done in the LabVIEW environment; by drawing.

The integration is done with a built-in integration block from the LabVIEW library (Time Domain Math Block). Labview operates on discrete signals (as all digital computing environments), and the integration is approximated by a 3-point quadrature [1];

$$\int x(t)dt \approx \frac{1}{6}\sum_{j=0}^{n}(x_{j-1} + 4x_j + x_{j+1})\delta t.$$

For detailed information on each block see the freely available LabVIEW documentation on the internet.

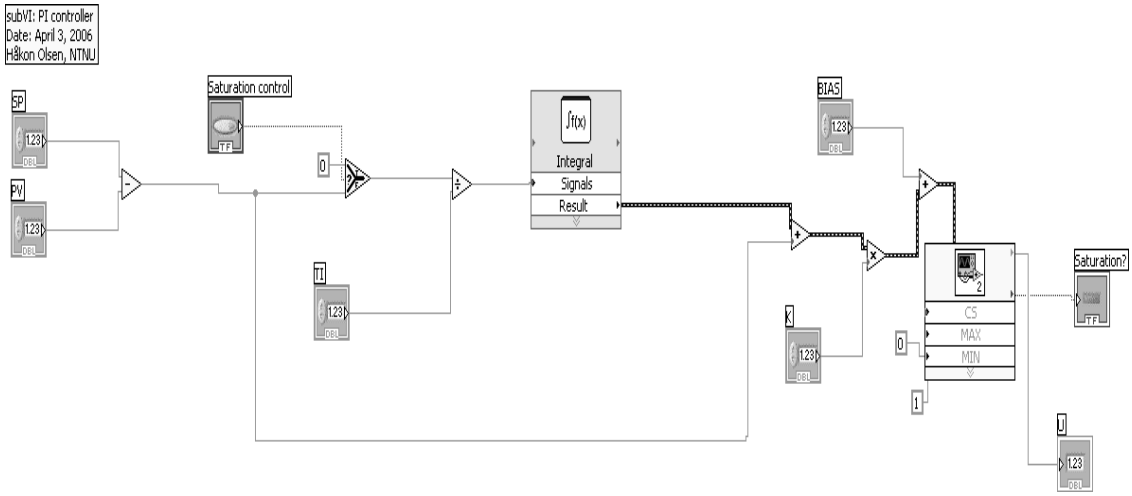

Figure A.1: PI Controller implementation.

Saturator

The saturator is a sub VI used to ensure that the signal sent to the hardware is within the allowable range. If a labview program tries to send a signal outside the allowable range to the hardware, the software stalls. The saturator takes as input a process variable and max and min limits. If the process variable is outside the allowable range, the saturator resets the signal to the nearest limit. The outputs from the saturator are the process signal (possibly reset to the given range limit) and a boolean signal used by other program components to tell if the process variable is saturated.

Measurement

The measurement VI takes the signals sent from the hardware and transforms them to human-readable form. The signal inputs are in the RS-232 standard range (either 0-5 V dc voltage or 0-24 mA current). Factory calibrations are used and the instruments are considered linear in their respective reliable ranges. The mathematical expressions are written in text form into C language formula nodes.

[1] Source: *http://www.ni.com*.

MATLAB Files

The model was available from Espen Storkaas's work and can be downloaded from the following web page; *http://www.chemeng.ntnu.no/ skoge*. The Matlab files used in this work are basically the same as on that page, but with parameters and geometrical description changed to fit the laboratory plant.

Appendix B

Model Parameters (Tuning)

This chapter gives the parameters used in the Storkaas model for designing the controllers in Chapter 4 (Cascade Control). For significance of the parameters, please refer to the original work (Storkaas, 2005)

```
%All units are standard SI when not given below.
data.r=0.0195/2;                 %Pipe radius
L1=3;                            %Feed pipe length
FG=0.8;                          %Liquid fraction in feed pipe
data.V_G1=pi*data.r^2*L1*(1-FG); %Compressible volume upstream bend
data.V_G1=3.2*(data.V_G1+(0.315*pi*0.11^2/4));
data.rho_L=998;                  %Liquid density
data.theta=0.0087;               %Feed pipe inclination towards bend
data.A2=data.r^2*pi;             %Riser cross sectional area
data.H1=2*data.r/cos(data.theta);%Max liquid height low-point
data.H2=2.8;                     %Riser height
data.H3=2*data.r;                %Pipe diameter
data.L3=0.1;                     %Pipe length from riser to valve
data.A1=data.A2/sin(data.theta); %Cross sectional area upstream riser
data.A3=data.H3*data.L3;         %Cross sectional area upstream choke
data.R=8314;                     %Universial gas constant J/(K*Kmol);
data.T=298;                      %Temperature K
data.M_G=28.9;                   %Molecular weight of gas kg/Kmol;
data.g=9.81;                     %Gravitational acceleration
data.P0=1.013e5;                 %Separator pressure
data.V_T=data.A2*data.H2+data.A3*data.H3; %Riser volume
data.n=0.705; %2.55;             %Tuning parameter for entrainment equation
```

Appendix C

Experimental Results

This appendix summarizes some experimental results on anti-slug control.

Open Loop

The following data charts show the results from experiments used for tuning the model. The data were obtained before the mini-loop was rebuilt, such that the accuracy of the tuning based on these data may be questionable. The results are reproduced in Figures C.1 to C.3.

Top-side Feedback Control

This section shows a few experimental charts. The first one is from an experiment with cascade control, where a flow estimate is used in the inner loop with gain 0.35 and top-side pressure in the outer loop with gain -0.5 and integral time 100. The stabilization was successful and gave a very steady pressure trajectory. The pressure chart is shown in Figure C.4.

The use of bottom-side pressure as indicator for controller performance when using top-side measurement is recommended because the signal is much less distrubed by noise. This is natural, because the noise creating element is the control valve, and the noise has to propagate through the whole riser and tube up till the pressure measurement. This capacity has considrable damping effect.

An experiment with gain scheduling and top-side control was also done, to see if varying the bias could help stabilize the flow using a flow measurement only (or really an estimate of the flow). The result is shown in Figure C.5. Gain scheduling may be used in combination with multivariable control to improve performance.

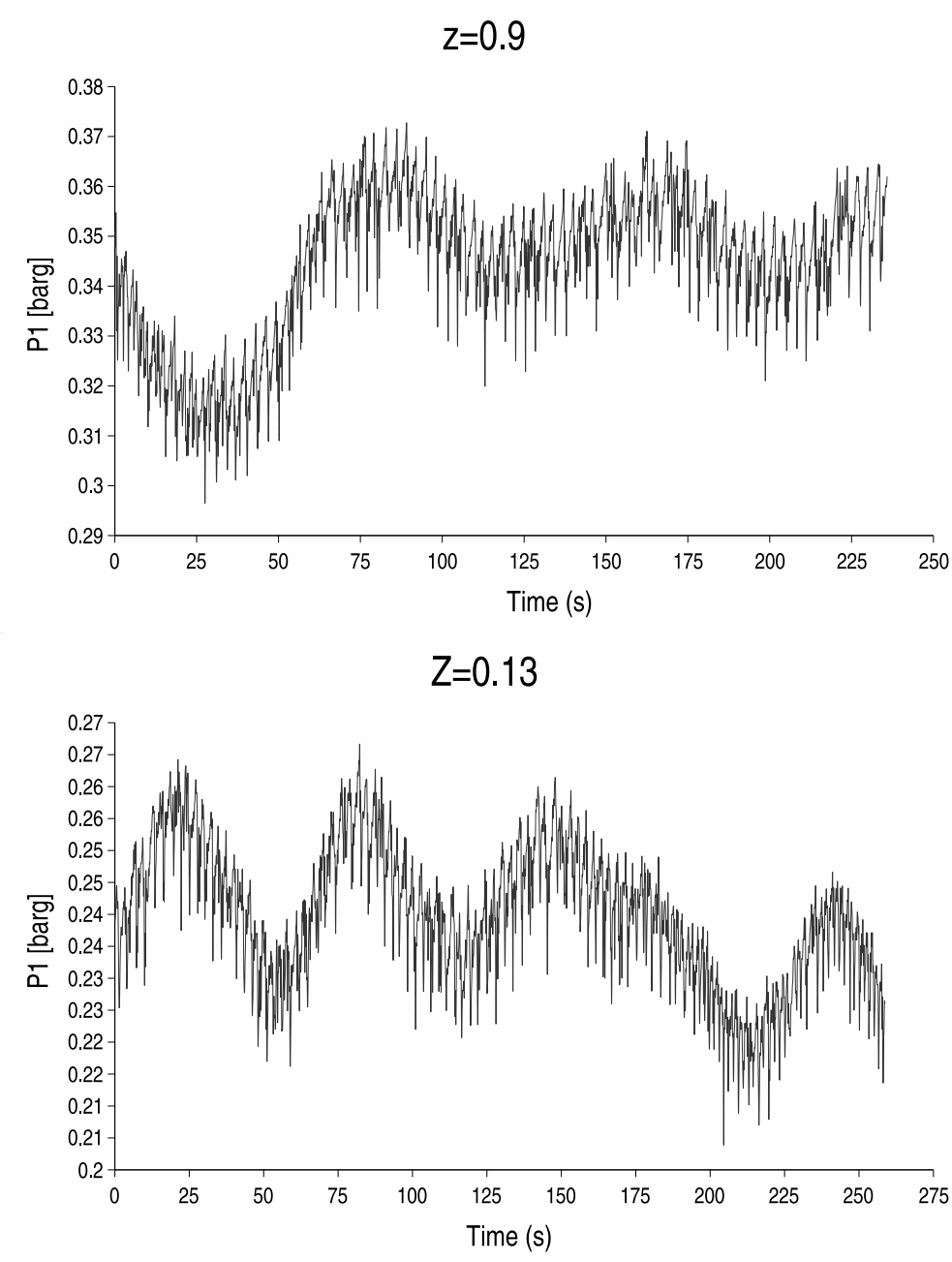

Figure C.1: Open loop vave openings 9 and 13%.

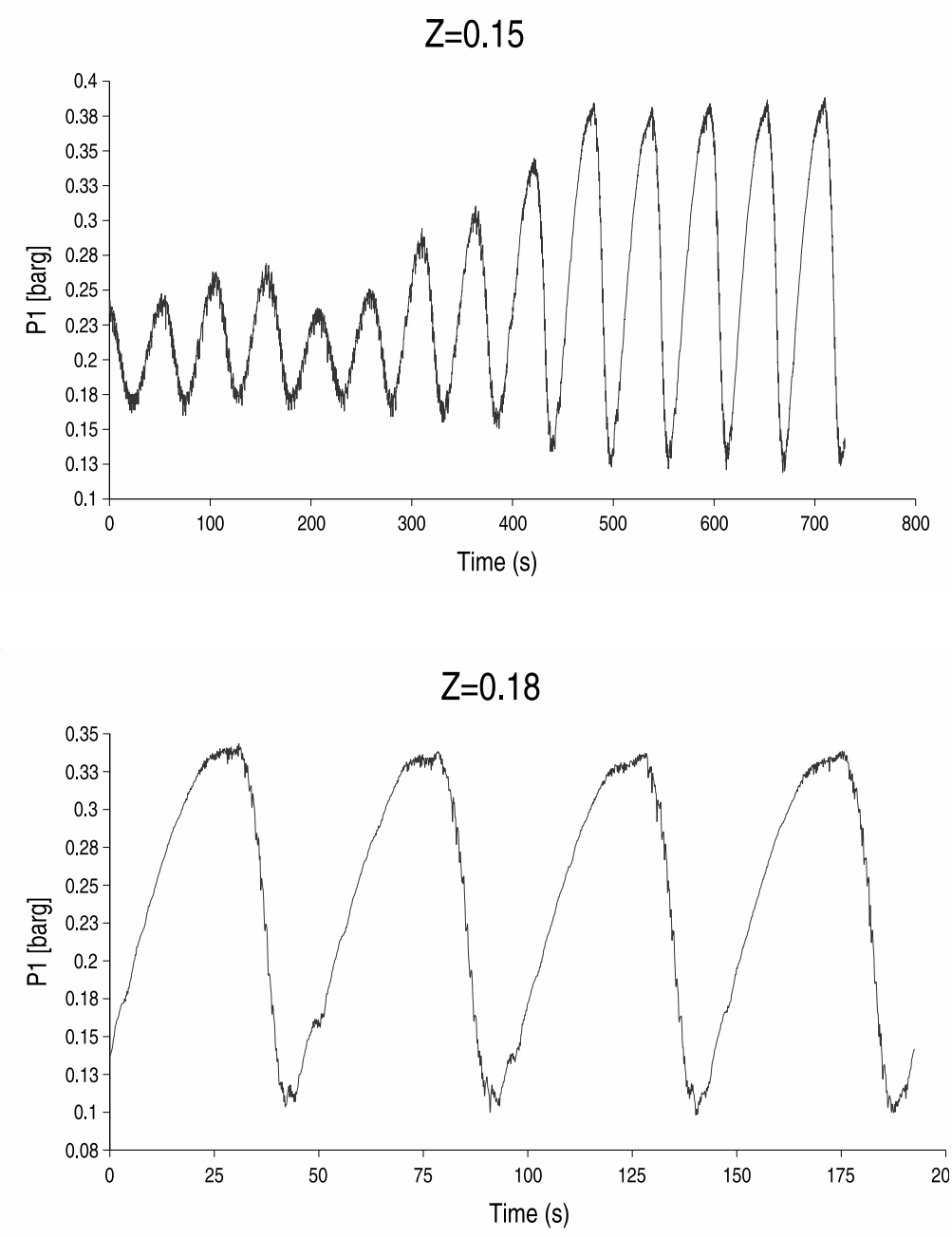

Figure C.2: Open loop vave openings 15 and 18%.

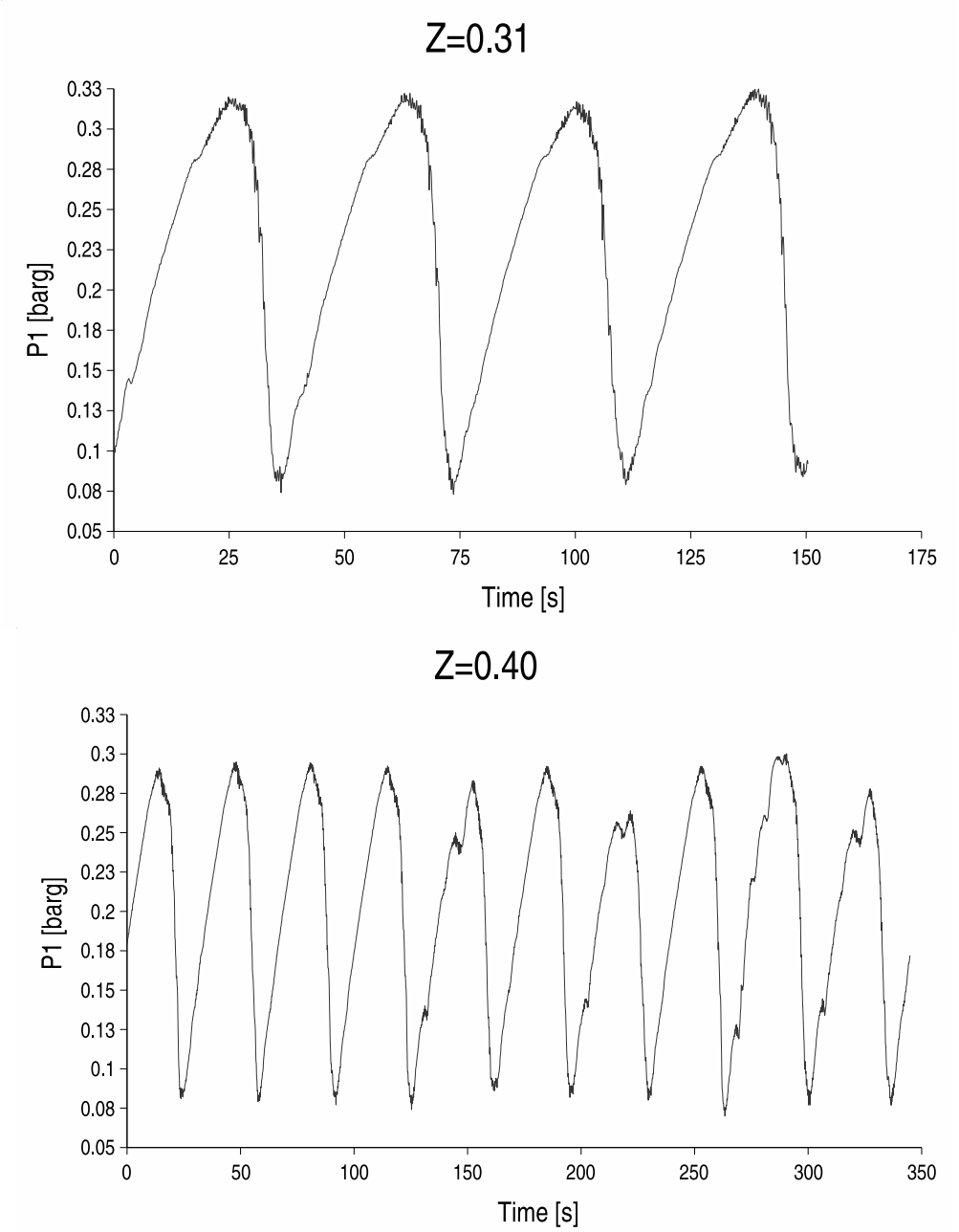

Figure C.3: Open loop vave openings 31 and 40%.

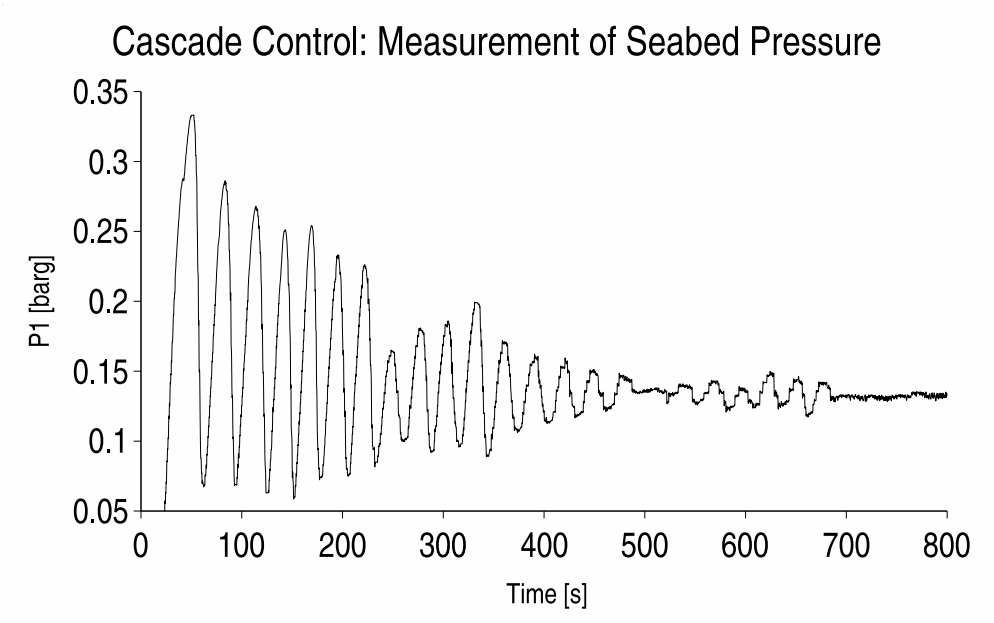

Figure C.4: The bottom pressure is a good indicator of controller performance. This is the seabed pressure chart when the flow is stabilized by Q in the slave loop and P_2 as controlled variable in the master loop.

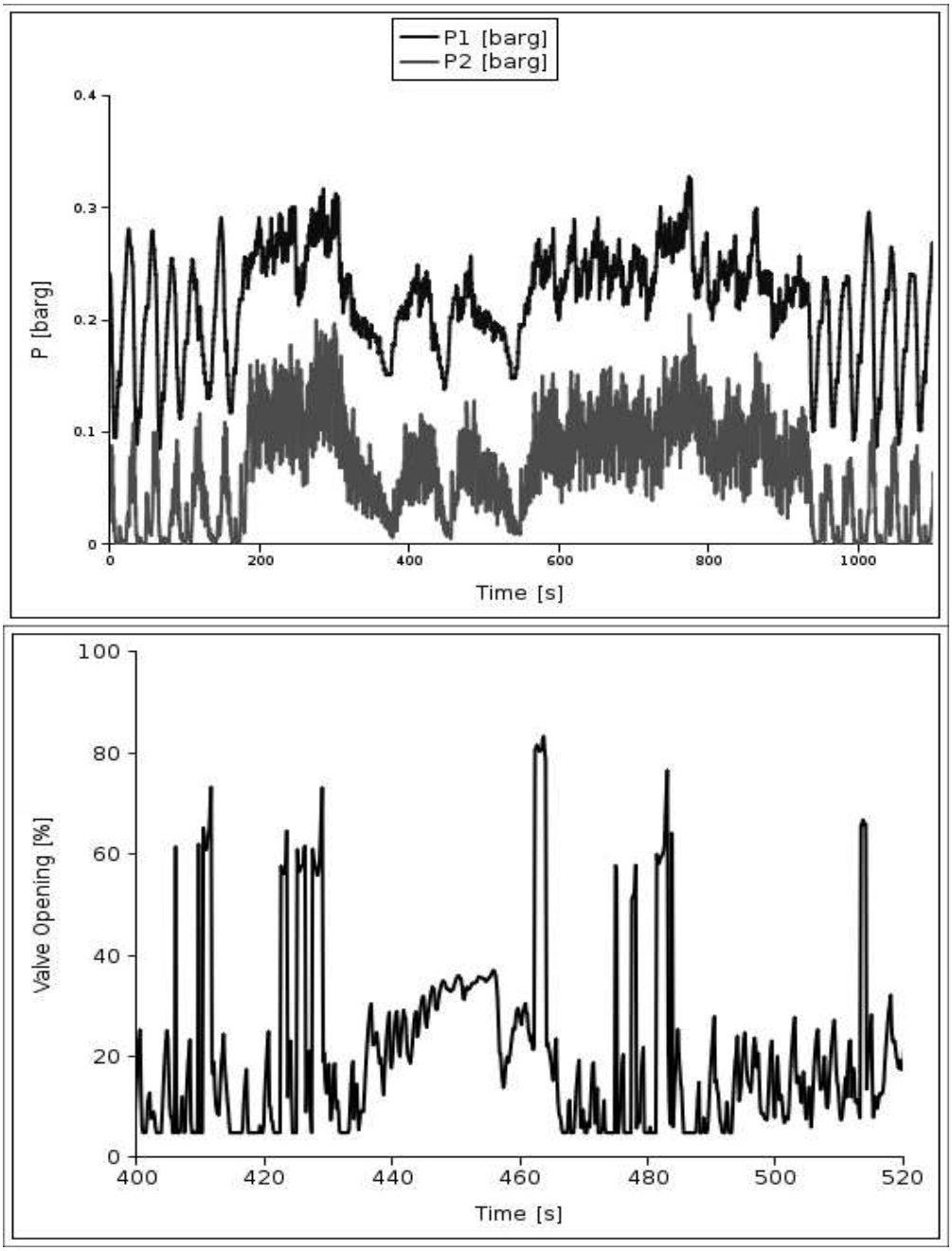

Figure C.5: Gain scheduling does help in stabilizing the flow, but due to zeros close to the imaginary axis in the transfer function from valve opening to flow measurement, drift seem unavoidable.

Appendix D

Numerical Considerations for Simulations in MATLAB

The Storkaas model is a rather complex differential-algebraic model with several hard nonlinearities of the following type;

$$\begin{aligned} &\text{If } \theta > \theta_1 \\ v = Kf(\theta)z\sqrt{\frac{P-P_0}{\rho}}, \\ &\text{else} \\ v = 0, \end{aligned} \tag{D.1}$$

where θ is some model parameter. This kind of nonlinearity may lead to very large and fast changes in state derivatives. This again, may lead to numerical instability. This is not a problem when the model is in such a state that the parameter does not vary a lot; that is, when the system has been stabilized. This is a reason why a variable step-length method is crusial in this kind of simulations.

Another "feature" of the model, is that it resides in a differential-algebraic form. The solution of Index-1 DAE problems may lead to very stiff problems. Matlab offers two routines for solving stiff problems and problems on DAE form; the ODE23T routine and the ODE15S routine. Experience has shown that the ODE23T routine is faster for the Storkaas model.

The DAE routines for use in the Matlab environment take as input models on the form

$$M(x,t)\frac{dx}{dt} = f(x,t). \tag{D.2}$$

The Storkaas model has a constant mass matrix with a zero row for the algebraic state. The algebraic state in the model is the mixture density in the riser. Hence, the mass matrix is a constant singular square matrix. The problem with the DAE formulation occurs when the problem is implemented in an S-function for inclusion in Simulink models; Simulink does not have any obvious way of utilizing the mass matrix notation. Therefore, the calculation of the algebraic state is done iteratively by letting the variable be persistent in the S-function. This works well as long as the density does not change too fast. When the gas flow rate fed to the system is very low (or really, the ratio of gas input to liquid input), the system becomes very

stiff and the resulting oscillations take the form of relaxation oscillations. Such systems are characterized by extremely fast changes in state. In our case, this means a large change in mixture density may happen in a shorter time interval than the minimum time step used by the integration method. Matlab will then most often stall with the following exit information;

```
Unable to meet integration tolerances without reducing the step size
below 1E-10.
```

Therefore, it is important to investigate the stiffness properties when numerical problems occur in Simulink. Adding some extra dynamics may be a possible option (it would not allow infinite rates of change in physical variables).

Bibliography

A. Baardsen. Anti-slug control: Experimental verification. Technical report, Norwegian University of Science and Technology, 2003.

J.-M. Godhavn, M. P. Fard, and P. H. Fuchs. New slug control strategies, tuning rules and experimental results. *Journal of Process Control*, 15:547–557, 2005.

D. E. Seborg, T. F. Edgar, and D. A. Mellichamp. *Process Dynamics and Control*. John Wiley & Sons, NJ, USA, 2nd. edition, 2004.

S. Skogestad and I. Postlethwaite. *Multivariable Feedback Control*. John Wiley & Sons, UK, 2005.

E. Storkaas. *Anti-slug control in pipeline-riser systems*. PhD thesis, Norwegian University of Science and Technology, 2005.

F. Verhulst. *Nonlinear Differential Equations and Dynamical Systems*. Springer-Verlag, Berlin, 1990.

N. Young. *An Introduction to Hilbert Space*. Cambridge University Press UK, 1988.